FINAL PROJECT REPORT TO

NASA LEWIS RESEARCH CENTER

ELECTROCATALYSIS OF FUEL CELL REACTIONS: INVESTIGATION OF ALTERNATE ELECTROLYTES

January 1, 1982 - December 31, 1983

Der-Tau Chin (Principal Investigator)

K-L. Hsueh (Research Assistant)

H.H. Chang (Research Assistant)

Department of Chemical Engineering

Clarkson College of Technology

Potsdam, New York

(NASA-CR-173261) ELECTROCATALYSIS OF FUEL CELL REACTIONS: INVESTIGATION OF ALTERNATE ELECTROLYTES Final Report, 1 Jan. 1982 - 31 Dec. 1983 (Clarkson Coll. of Technology) 63 p HC A04/MF A01 CSCL 10A G3/44

N84-20013

Unclas 12480

SUMMARY

This work is concerned with a study of oxygen reduction and transport properties of the electrolyte in the phosphoric acid fuel cell. The areas covered in the work were: (i) development of a theortical expression for the rotating ring-disk electrode technique; (ii) determination of the intermediate reaction rate constants for oxygen reduction on platinum in phosphoric acid electrolyte; (iii) determination of oxygen reduction mechanism in trifluoromethanesulfonic acid (TFMSA) which has been considered as an alternate electrolyte for the acid fuel cells; and (iv) the measurement of transport properties of the phosphoric acid electrolyte at high concentrations and temperatures.

(1) Theoretical Analysis of the Rotating Ring-Disk Electrode Method

The previous theoretical treatments of the rotating ring-disk electrode method to distinguish between the mechanisms of electroreduction of O_2 to H_2O with and without the formation of H_2O_2 as an intermediate, were examined. A new expression was derived for $I_{dl}/(I_{dl}-I_d)$ as a function of $\omega^{-1/2}$ (where I_{dl} is the disk limiting current, I_d is the disc current and ω is the rotational speed of electrode) for five possible reaction models. This, along with the corresponding expressions for I_d/I_r vs. $\omega^{-1/2}$ (I_r is the ring current), enables the calculations of the individual rate constants for the intermediate steps of O_2 reduction. The experimental data of I_d and I_r were obtained for O_2 reduction on platinum in 0.55 M H_2SO_4 at 25°C. By use of these experimental results in the present theoretical treatment, it is shown that: (1) the most applicable model over the entire potential region was the one suggested by Damjanovic, Genshaw and Bockris: (2) the models involving the adsorption/desorption of H_2O_2 were applicable only over a narrow region of

potential: and (3) the models involving the chemical decomposition of H_2O_2 were inconsistent with the dependence of $I_{dl}/(I_{dl}-I_d)$ vs. $\omega^{-1/2}$.

(2) Oxygen Reduction in Phosphoric Acid

The oxygen reduction reaction was investigated at platinum electrodes in phosphoric acid in the concentration range 0.7M (6.6%) to 17.5M (95%) at 25°C using the rotating ring-disc electrode technique. The mechanism of the oxygen electrode reaction was discussed in terms of the direct four-electron transfer reduction to water and the formation of hydrogen peroxide as an intermediate in a parallel two-electron transfer reaction. The rate constants of the intermediate reaction steps were calculated from the ring-disc data for various potentials and electrolyte concentrations. The characteristics of the reaction were found to be markedly dependent on the concentration of phosphoric acid.

(3) Oxygen Reduction in TFMSA

Trifluoromethane sulfonic acid (TFMSA) has been considered as an alternate electrolyte for fuel cell applications. The kinetics of oxygen reduction at Pt was studied using a rotating ring-disc electrode technique in TFMSA (0.05, 0.1, 1.0, and 6.0M) and in 1.0M TFMSA with phosphoric acid additive (0.003 and 0.1M). The amount of hydrogen peroxide intermediate produced in TFMSA on oxide-covered Pt surface (electrode potential scanned from 1.0 to 0.3 V vs. RHE) was found to be higher than that on oxide-free surface (electrode potential scanned from 0.3 to 1.0 V vs. RHE). A half reaction order with respect to oxygen was observed for the oxygen reduction in TFMSA solutions. The reaction order increased to one with the addition of phosphoric acid to 1.0 M TFMSA. A possible mechanism of oxygen reduction was proposed to explain the half reaction order with respect to oxygen.

(4) Transport Properties of Phosphoric Acid Electrolyte

The transport properties of phosphoric acid are important to the fuel cell performances. In this work, the kinematic viscosity and specific conductivity of the electrolyte, have been measured over a range of phosphoric acid concentrations from 0.5 to 19 M (6 - 100%) and temperatures from 25 to 200°C. The specific conductivity was measured with a Beckman conductivity bridge and a conductivity cell. The kinematic viscosity was measured with Cannon-Fenske viscometers. The results indicate that the conductivity in concentrated phosphoric acid follows a non-Stokian transport mechanism.

ACKNOWLEDGEMENT

(1) This project was supported by a NASA Grant NAG 3-238. The grant originally covered the period, January 1 - December 31, 1982. The project was extended to December 31, 1983 with a no-cost extension.

(2) This work was carried out in collaboration with Dr. S. Srinivasan, the principle investigator on the DOE sponsored program ''Electrocatalysis of Fuel Cell Reactions'' at Los Alamos National Laboratory, Los Alamos, NM, 87544. The authors gratefully acknowledge his help and contributions to the project.

(3) The contribution of K-L. Hsueh was in partial fulfillment of the requirement of his Ph.D. degree in Chemical Engineering from Clarkson College of Technology. His experimental work, a part of theortical analysis and part of dissertation writing were carried out at Los Alamos National Laboratory while he was a graduate research associate during the period May 1981 - August 1982. He received a Ph.D. degree from Clarkson College in 1983. A copy of his dissertation abstract is attached in the appendix.

(4) The contribution of H.H. Chang is in partial fulfillment of a M.S. degree in Chemical Engineering from Clarkson College of Technology. A part of his experimental work was carried out at Los Alamos while he was a guest research assistant during the period June - August, 1982. He was supported by a Clarkson teaching assistantship during the period of January - August, 1983. He will complete his M.S. degree in May, 1984.

TABLE OF CONTENTS

I. INTRODUCTION

The energy crisis of 1973 stimulated the renaissance of fuel cells (1). Fuel cells are superior to other electricity generators in several respects (2); such as: high efficiency, pollution free and silent operation. In fuel cells, the fuels are converted to hydrogen-rich gases and then fed into the fuel cell. The direct current generated from the cell is converted to alternating current by the power conditioner. The heat released from the fuel cell is utilized for the endothermic reaction in the fuel processor.

The essential criteria for fuel cells are dependent on the types of applications. The requirements for civilian terrestrial use are high efficiency, high power density, low capital cost and long life. The phosphoric acid fuel cell (3) appears to be the best candidate when natural gas and naphtha are used as fuels. This fuel cell is operated at 200°C and there is a need to transfer waste heat from the fuel cells to the fuel processor. Molten carbonate (1,4) and solid electrolyte (1,5) fuel cells appear to be promising when coupled with a coal gasifier operating at temperatures of 1000 ~ 1500°C.

The major cause of the efficiency loss in the fuel cell is due to the slow reaction rate of oxygen reduction at the cathode (8). The overpotential of the hydrogen electrode is less than 20 mV at 200 mA/cm^2; however, the overpotential of the oxygen electrode is 400 mV at the same current density. The oxygen electrode reaction is the major cause of efficiency loss in phosphoric acid fuel cells. It has been shown that the overpotential loss for the oxygen reduction reaction can be reduced with additives, such as, trifluoromethane sulfonic acid (TFMSA) into phosphoric acid electrolyte. The exchanging current density in aqueous TFMSA is one hundred times higher than

that in 85% H_3PO_4. The mechanism of oxygen reduction in H_3PO_4 and TFMSA is not known. The objective of this work are:

i) Study of electrode kinetics of oxygen reduction in fuel cell electrolytes- The reduction of oxygen involves two parallel reaction paths. One reaction path is the direct reduction of oxygen to water. The second path is the reduction of oxygen to hydrogen peroxide, followed by the reduction of hydrogen peroxide to water. An evaluation of the rate constants of individual reaction path of oxygen reduction is essential for the understanding of oxygen reduction kinetics. A method to calculate these rate constants from the rotating ring-disk experiment has been developed in this work. The kinetics of oxygen reduction was studied by using the rotating ring-disk electrode technique in phosphoric acid and trifluoromethanesulfonic acid (TFMSA). The results are summarized in this report.

ii) Investigation of transport properties of phosphoric acid electrolyte- The physical properties of electrolyte are important to the fuel cell performance (3). The conductivity of the electrolyte can affect the cell IR loss. The maximum operating temperature is limited by the boiling point of the electrolyte. Besides, the rate of oxygen reduction is proportional to the solubility and diffusivity of dissolved oxygen in the electrolyte (12). The information of transport properties in phosphoric acid over a wide concentration range would clearify the change in solvent structure (from water to phosphoric acid) when the electrolyte changes from aqueous solution to concentrated phosphoric acid medium. For these purposes, the conductivity and viscosity of phosphoric acid were measured over a range of concentrations from 0.7 to 17.5M (6.6 - 100%) and the temperature from 25 to 200°C.

II. ELECTRODE KINETICS OF OXYGEN REDUCTION

The aims of this work is to investigate the effects of the electrolyte on the kinetics of oxygen reduction at platinum. For this purpose, the rotating ring-disk electrode technique was used. All the kinetics studies were carried out on the platinum electrode because platinum is the best catalyst for the fuel cell reaction. Since the phosphoric acid is presently used in the fuel cell and trifluoromethanesulfonic acid (TFMSA) shows promise for fuel cell applications (13), the investigation was carried out in these two acids.

There are four sections in this chapter. In section 2.1, the experimental procedures and preparation of electrode, electrolytes, and glassware are described. In section 2.2, a set of new equations for the calculation of rate constants of the intermediate reaction steps from the rotating ring-disk electrode is developed. In section 2.3, the results for the reduction of oxygen in phosphoric acid over the concentration range of 0.7 - 17.5M are analyzed by the method presented in section 2.2. The results of oxygen reduction in aqueous TFMSA (0.05 ~ 6.0M) and in a mixed acid which containing 1.0M TFMSA and 0.003 ~ 0.1M phosphoric acid are presented in section 2.4.

2.1 EXPERIMENTAL

Experimental set-up

A glass cell with one compartment for the test and auxiliary electrodes and another for the reference electrode was used in the electrode kinetics experiments. A platinum ring-disk electrode (Pine Instrument) with a collection efficiency of 17.6% served as the working electrode. The electrode potentials were measured against a dynamic hydrogen electrode (DHE) and were converted to a reversible hydrogen electrode (RHE) scale. A large platinum gauze was used as the counter electrode. The potentials of the disk and ring electrodes were controlled by a potentiostat (Pine Instrument RDE 3) and the rotational speed of the electrode was controlled by an analytical rotator

(Pine Instrument ASR 2). The currents at the disk and ring electrodes were recorded on a dual pen X-Y-Y' recorder (Soltec 6431).

Preparation of electrolytes, gases, and glassware

The cell, the electrodes and the glassware were cleaned with chromic acid (0.1 mol. $K_2Cr_2O_7$ dissolved into 1 ℓ H_2SO_4) followed by soaking in a 1.1 H_2SO_4/HNO_3 solution for 8 hr. and then in double distilled water for another 8 hr. The 0.55M sulfuric acid was prepared by diluting concentrated sulfuric acid (ultra pure, Alfa, Ventron Div.) with double distilled water. Phosphoric acid (85%, electronic grade, J.T. Baker) was treated with 10% hydrogen perioxide (90%, stabilizer free, FMC) and heated to 50-70°C for 1 hr. The solution was concentrated to 85% by evaporation at 160°C in a Teflon vessel. The solution was diluted with double distilled water to the desired concentrations. Trifluoromethanesulfonic acid (3M Co.), was distilled twice under vacuum (B.P. < 40°C). The distillate was added to double distilled water to form trifluoromethanesulfonic acid (TFMSA) monohydrate which was then vacuum-distilled (B.P. < 80°C). Before use, the monohydrate was diluted with double distilled water to the desired concentration.

Experimental procedure

Before the electrode kinetics experiments, the solution was deaerated with purified nitrogen gas and a cyclic voltammogram on the platinum disk electrode was examined to insure the purity of solutions. Then the purified oxygen was bubbled through the electrolyte for 1 hr. During the rotating ring-disk electrode experiments, the potential of the disk electrode was scanned from 1.0 to 0.3 V vs. DHE at a scan rate of 5 mV/S, while the potential of the ring electrode was maintained at 1.1 V vs. DHE (this is a limiting current potential for the oxidation of hydrogen peroxide to oxygen). Experiments were carried out for a range of rotational speed from 400 to 4900 rpm at 20-25°C.

2.2 THEORETICAL ANALYSIS OF THE ROTATING RING-DISK ELECTRODE METHOD

The rotating ring-disk electrode technique has been extensively used for the investigation of the mechanism of the oxygen reduction in which hydrogen peroxide is formed as an intermediate (14-19). In this method, the reduction of oxygen takes place on a central disk electrode and the generated hydrogen peroxide is detected at a concentric ring electrode with a larger radius. The purpose of this work is to modify previous theoretical treatments (15,16,19) and to determine the rate constants of the intermediate steps for the reaction models shown in Fig. 1. The rotating ring-disk electrode experimental data obtained for oxygen reduction at platinum in 0.55M sulfuric acid are used to illustrate the procedure of the present theoretical analysis.

Modification of theoretical treatments for the calculation of rate constants

Based on the material balances, the mathematical expression which would permit the calculations of the rate constants of the intermediate steps for the oxygen reduction reaction can be derived for each of the models presented in Fig. 1. For the sake of brevity, only the equations for Model 1 are presented here. The details of the analysis are given in Reference 6 and 9.

From the material balance of oxygen and hydrogen peroxide species in Model 1 (Fig. 2.1), the relations among the ring current, I_r and the expressions for ring (I_r) and the disk current, I_d, the limiting current at the disk, I_{dl}, and the rotating speed of electrode, ω can be expressed as:

$$\frac{I_d}{I_r} = \frac{1}{N}\left[1+2\frac{k_1}{k_2}\right] + \left[\frac{2(k_1/k_2+1)}{N\ Z_2}k_3\right]\omega^{-1/2} \qquad (1)$$

$$\frac{I_{dl}}{I_{dl}-I_d} = 1 + \frac{k_1+k_2}{Z_1}\omega^{-1/2} \qquad (2)$$

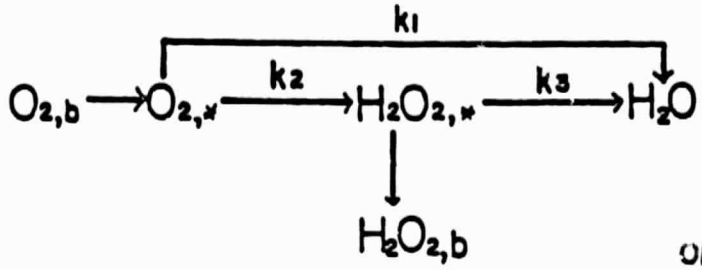

Model 1

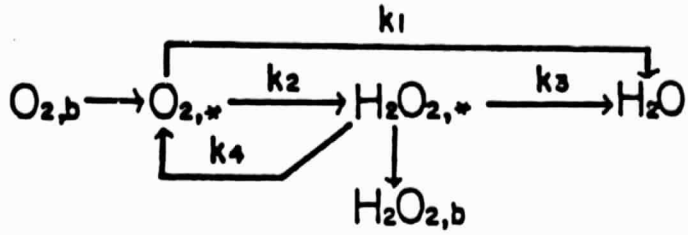

Model 2

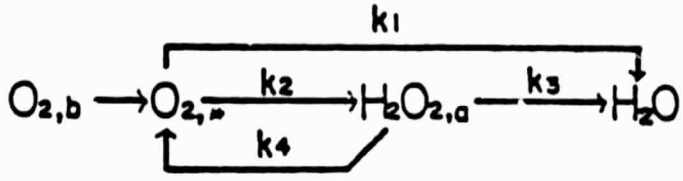

Model 3

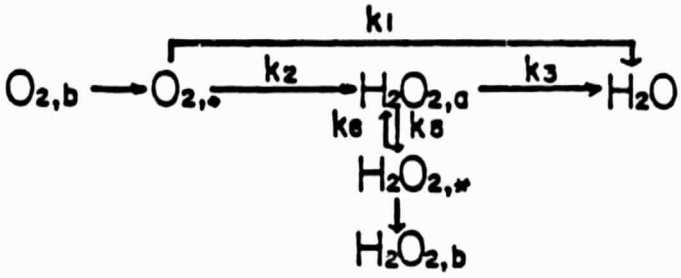

Model 4

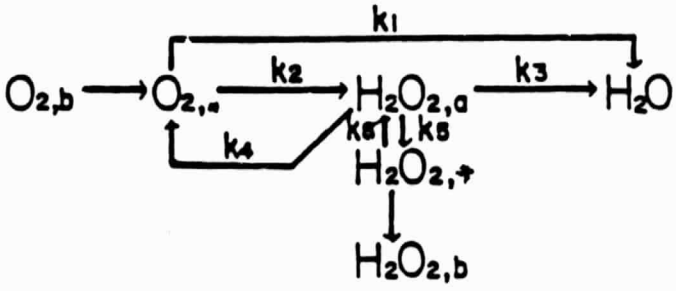

Model 5

Fig. 1 Reaction schemes for the electroreduction of O_2 considered in the present work.

Accordingly, the rate constants k_1, k_2, and k_3 may be determined from the intercepts and slopes of the plot of I_d/I_r vs. $\omega^{-1/2}$ and from the slopes of the plot of $I_{d1}/(I_{d1}-I_d)$ vs. $\omega^{-1/2}$ at different disk potential.

Evaluation of the rate constants

Two important expressions for the calculation of the rate constants are: (i) $I_{d1}/(I_{d1}-I_d)$ as a function of $\omega^{-1/2}$; and (ii) I_d/I_r as a function of $\omega^{-1/2}$. Figure 2 shows that the plot of $I_{d1}/(I_{d1}-I_d)$ vs. $\omega^{-1/2}$ at different electrode potentials exhibits a linear behavior with an intercept equal to 1. The plots of I_d/I_r vs. $\omega^{-1/2}$ at various electrode potentials are given in Fig. 3 (from 0.75 to 0.55 V vs. RHE) and in Fig. 4 (from 0.55 to 0.35 V vs. RHE). Using Model 1, it is possible to calculate the rate constants over the entire potential range (from 0.3 to 0.4 V vs. RHE); the rate constants in H_2SO_4 as a function of electrode potential are presented in Fig. 5. The ratio of k_1 to k_2 is about 5 ~ 12 and is potential-dependent. Since k_1 is larger than k_2, oxygen is mainly reduced to water via the direct four-electron transfer reaction path and only small amount of oxygen is reduced to water via the series reaction path which involves hydrogen peroxide as an intermediate. The rate constant k_3 is greater than k_2. This indicates that hydrogen peroxide is reduced to water at a relatively rapid rate. Therefore, only a little amount of hydrogen peroxide diffuses into the bulk electrolyte as evidenced by the small ring currents. The faradaic efficiency for oxygen reduction is about 97%.

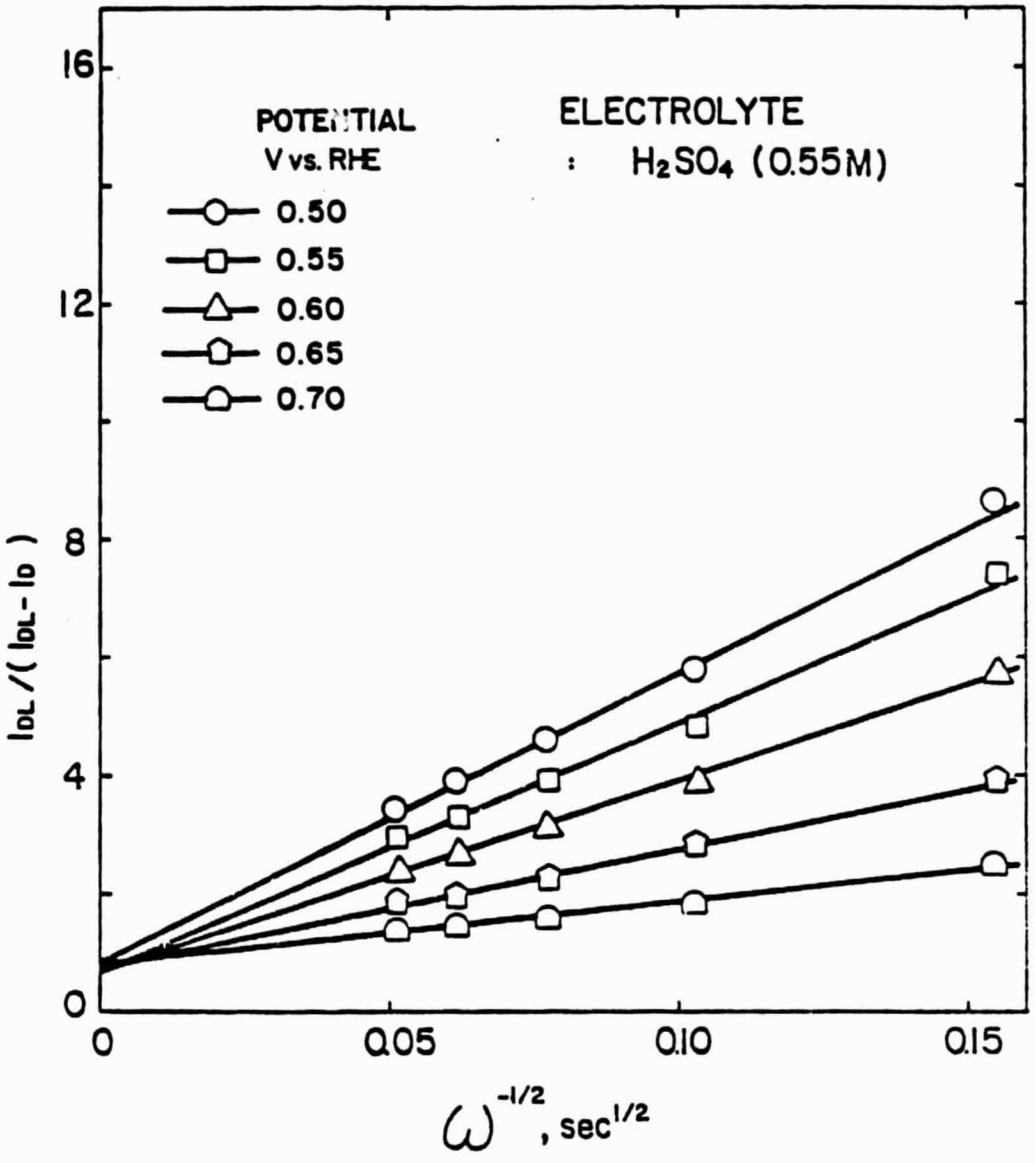

Fig. 2. $I_{dl}/(I_{dl} - I_d)$ as a function of $\omega^{-1/2}$ at various disc potentials.

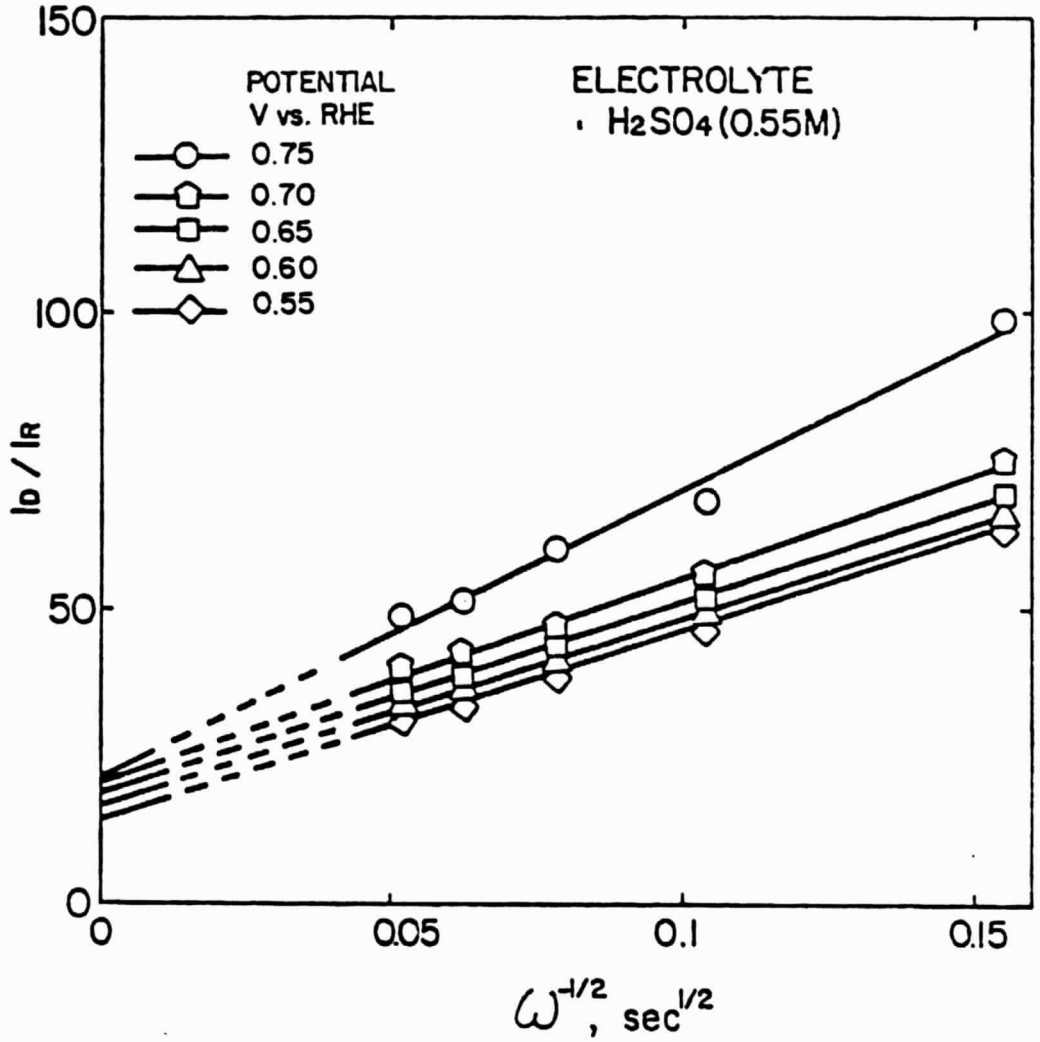

Fig. 3 I_d/I_r vs. $\omega^{-1/2}$ in the potential region 0.75 ~ 0.55, V vs. RHE

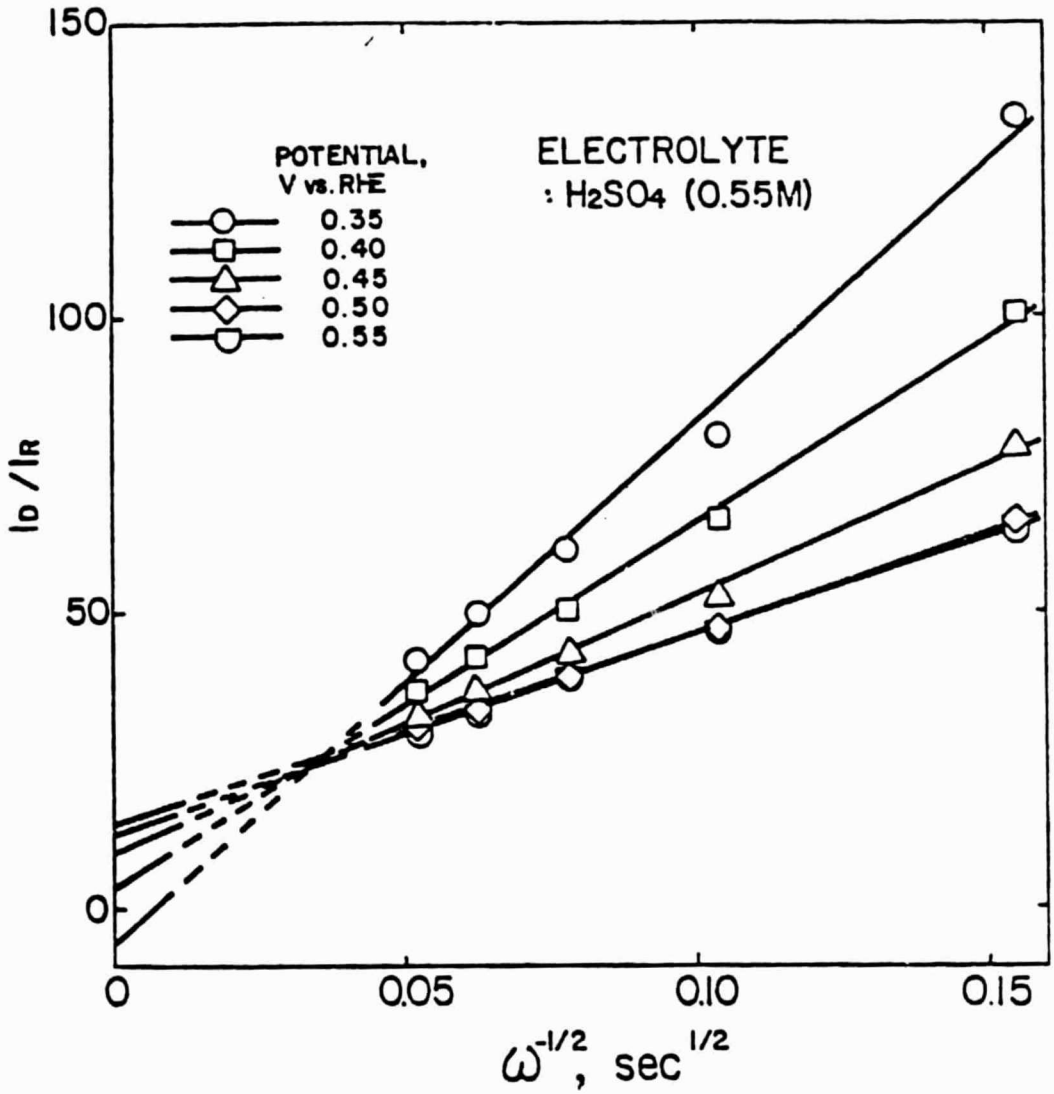

Fig. 4 I_d/I_r vs. $\omega^{-1/2}$ in the potential region 0.55 ~ 0.35, V vs. RHE

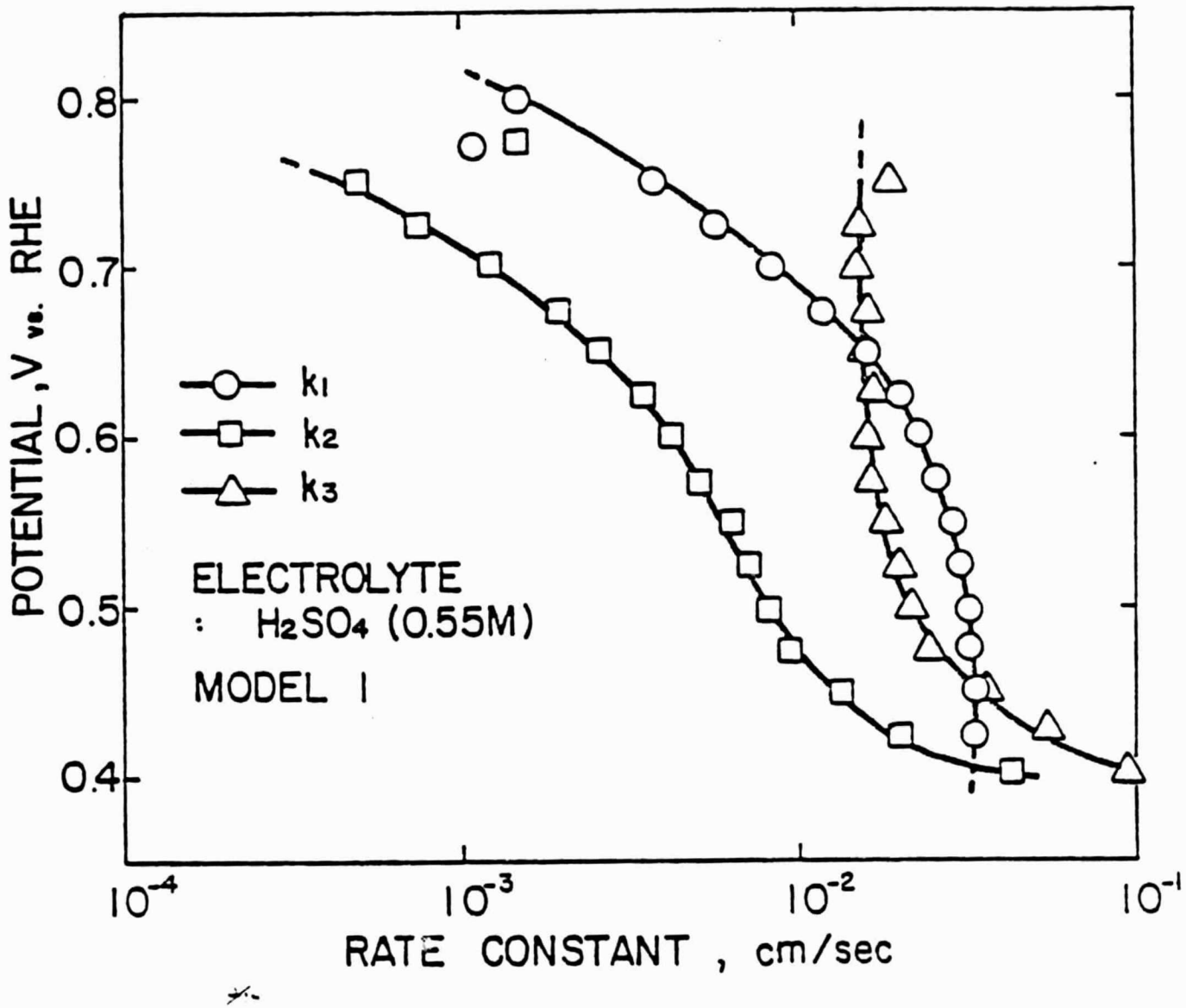

Fig. 5 Rate constants of intermediate steps for O_2 reduction on Pt in 1N H_2SO_4. These constants were calculated based on Model 1.

2.3 KINETICS OF OXYGEN REDUCTION AT PLATINUM IN PHOSPHORIC ACID

Concentrated phosphoric acid is presently used as the electrolyte in advanced fuel cells. The factor limiting the efficiency of this fuel cell is the overpotential for oxygen reduction reaction. The structure and physical properties of concentrated phosphoric acid are not well understood, but these certainly play a role in the kinetics of the oxygen reduction reaction. The double layer of mercury/concentrated phosphoric acid interface is thicker than in aqueous media (20). It is resonable to assume that there is a transition of the interfacial and bulk properties when the electrolyte concentration increases from a water-based to a phosphoric acid-based solvent structure. For this reason, the present study was undertaken to elucidate the effect of the concentration of phosphoric acid solutions (from 0.7 to 17.5M) on the kinetics of oxygen reduction at platinum electrodes.

Mass Transfer-Corrected Tafel Behavior

A rotating ring-disk electrode was used to measure the polarization curves of oxygen reduction at platinum, and to quantitatively determine the amount of the hydrogen perioxide intermediate formed during the reduction process. The mass transfer corrected Tafel behavior for oxygen reduction on platinum for different phosphoric acid concentrations is shown in Fig. 6. The plots correspond to the equation

$$E = \frac{2.3RT}{\alpha F} \log I_o - \frac{2.3RT}{\alpha F} \log \frac{I_{dl} I_d}{I_{dl} - I_d} \qquad (3)$$

The Tafel plots presented in Fig. 6 are independent of rotation speed. In the region from 0.6 to 0.8 V vs. RHE, the Tafel slopes are about 120 mV. This result is similar to that (12,21,22) in other acid media. This indicates that the overall reduction of oxygen is controlled by the first charge transfer step under the Langmuir adsorption condition.

Mechanistic Aspects of Electroreduction of Oxygen

Based on Model 1 and the procedure illustrated in the method the preceding theoretical analysis section, the values of k_1, k_2, and k_3 for oxygen reduction in phosphoric acid have been calculated. The rate constants (k_1, k_2, and k_3) are presented as a function of electrode potential for various phosphoric acid concentrations in Fig. 7-10. In all cases, the ratio k_1/k_2 is greater than 10, implying that most of oxygen reduces to water directly through the four electron transfer reaction.

From Fig. 7 to 9, it is apparent that for phosphoric acid concentrations up to 8M, k_2 has the same potential-dependence as k_1. This means that the rate determining step is probably the same for the both reaction paths. At higher concentrations, k_2 becomes independent of potential; this indicates that the rate of the reaction is controlled by a chemical step prior to the electron transfer step.

The behavior of k_3 is similar to that of k_2; it decreases with increasing phosphoric acid concentration. The significant decrease in k_2 and k_3 with increasing phosphoric acid concentration leads to an increase in the faradaic efficiency for the reduction of oxygen to water. This is important because at the high phosphoric acid concentrations used in the fuel cells, the amount of hydrogen peroxide formed during the operation is negligible.

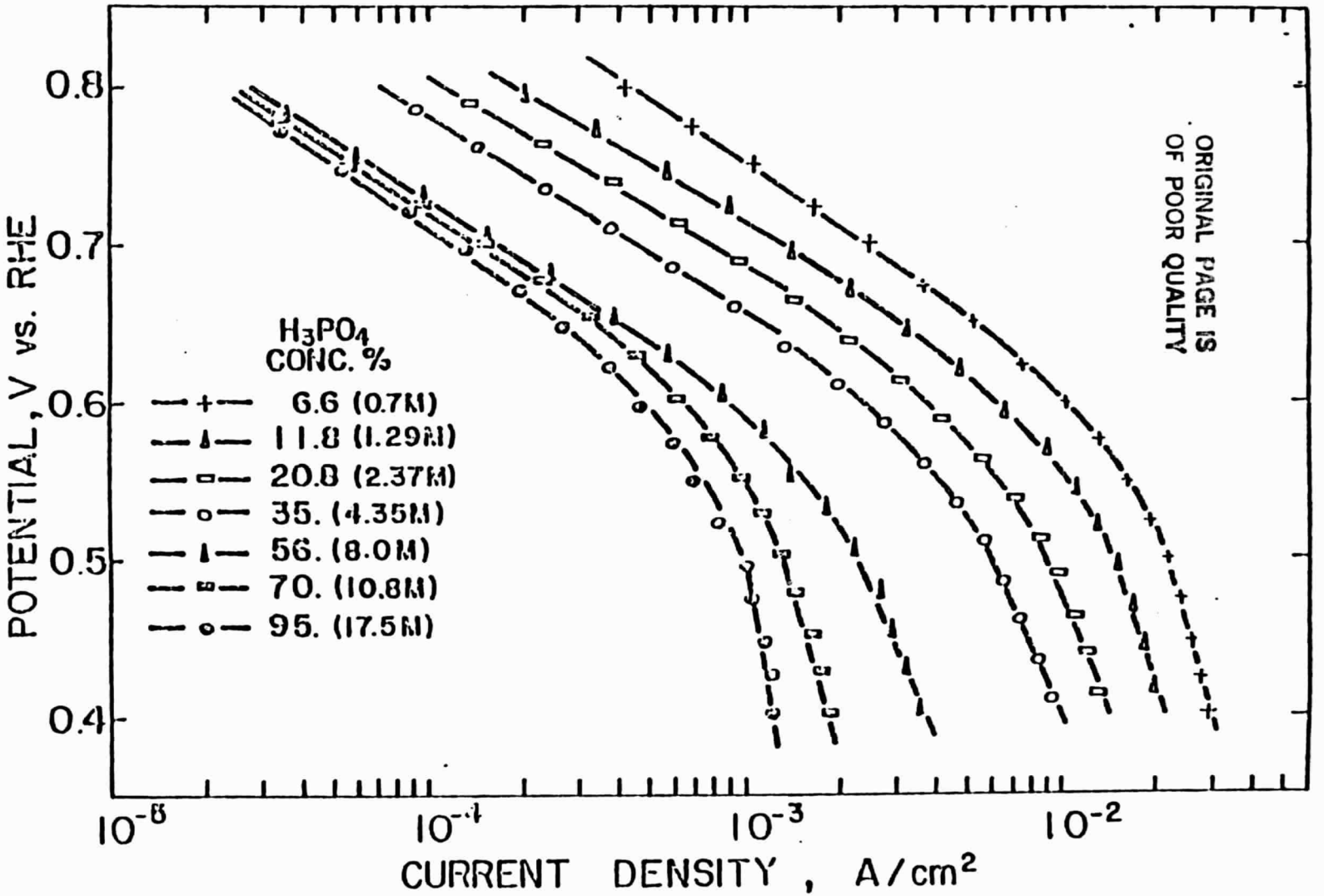

Fig. 6 Mass-transfer-corrected Tafel behavior for oxygen reduction on Pt in H_3PO_4 over the concentration range 6.6 to 95 w/o at 25°C. Tafel behavior is independent of electrode rotating speed in the 400- to 3600-rpm region.

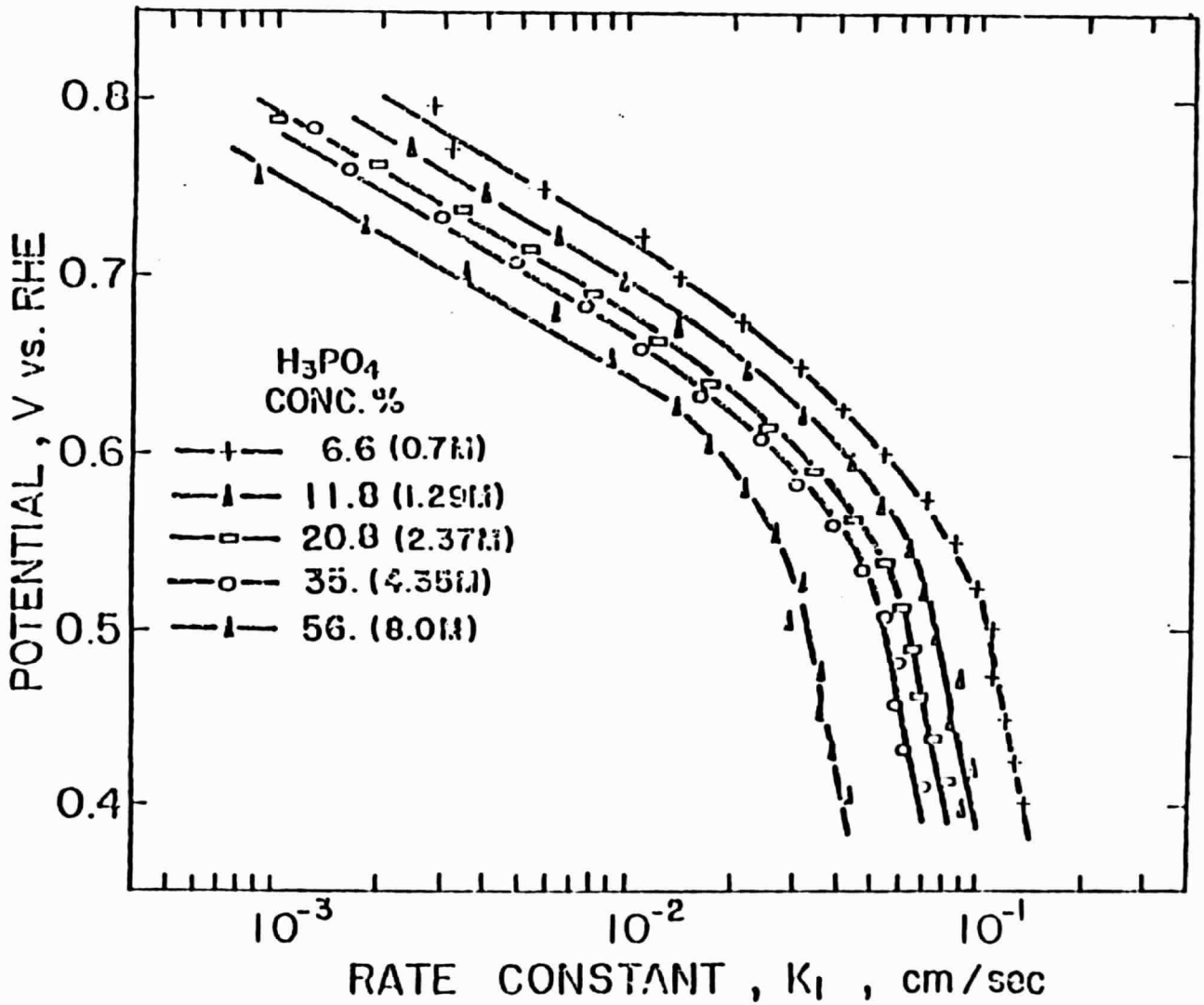

Fig. 7 Potential dependence of rate constant k_1 for oxygen reduction at Pt in H_3PO_4 in the concentration range 6.6 to 56 w/o at 25°C.

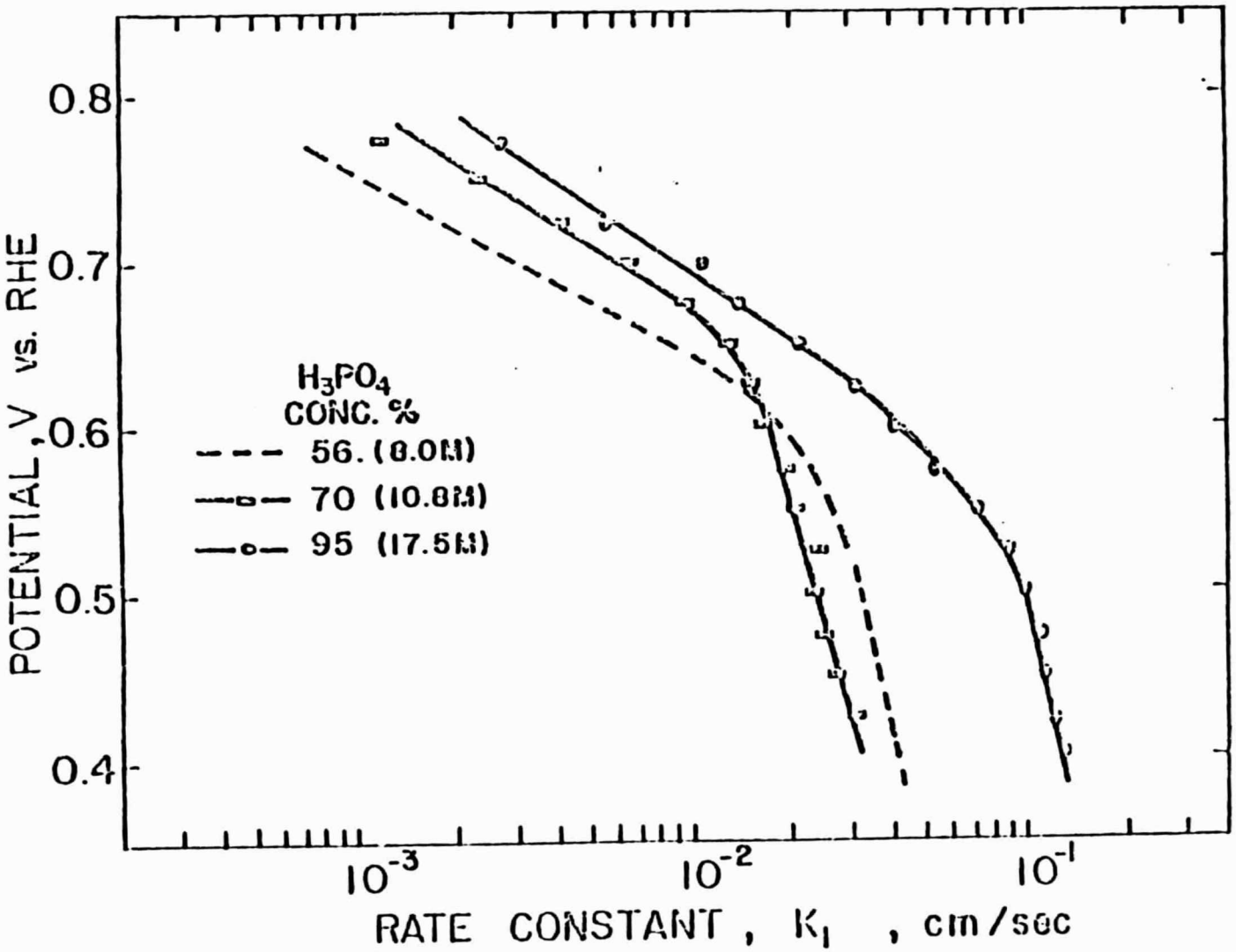

Fig. 8 Potential dependence of rate constant k_1 for oxygen reduction at Pt in H_3PO_4 in the concentration range 56 to 95 w/o at 25°C.

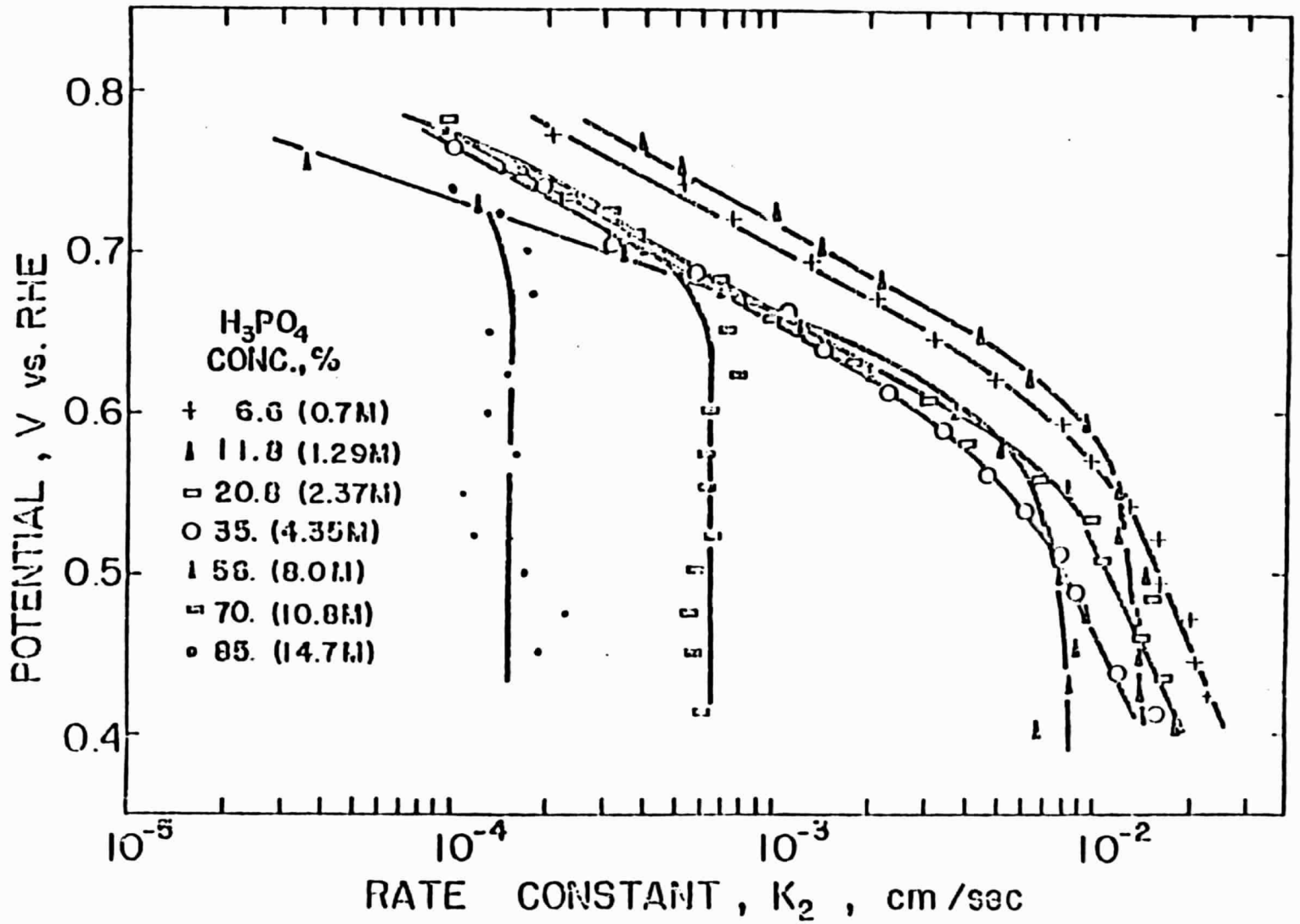

Fig. 9 Potential dependence of rate constant k_2 for oxygen reduction at Pt in H_3PO_4 in the concentration range 6.6 to 85 w/o at 25°C.

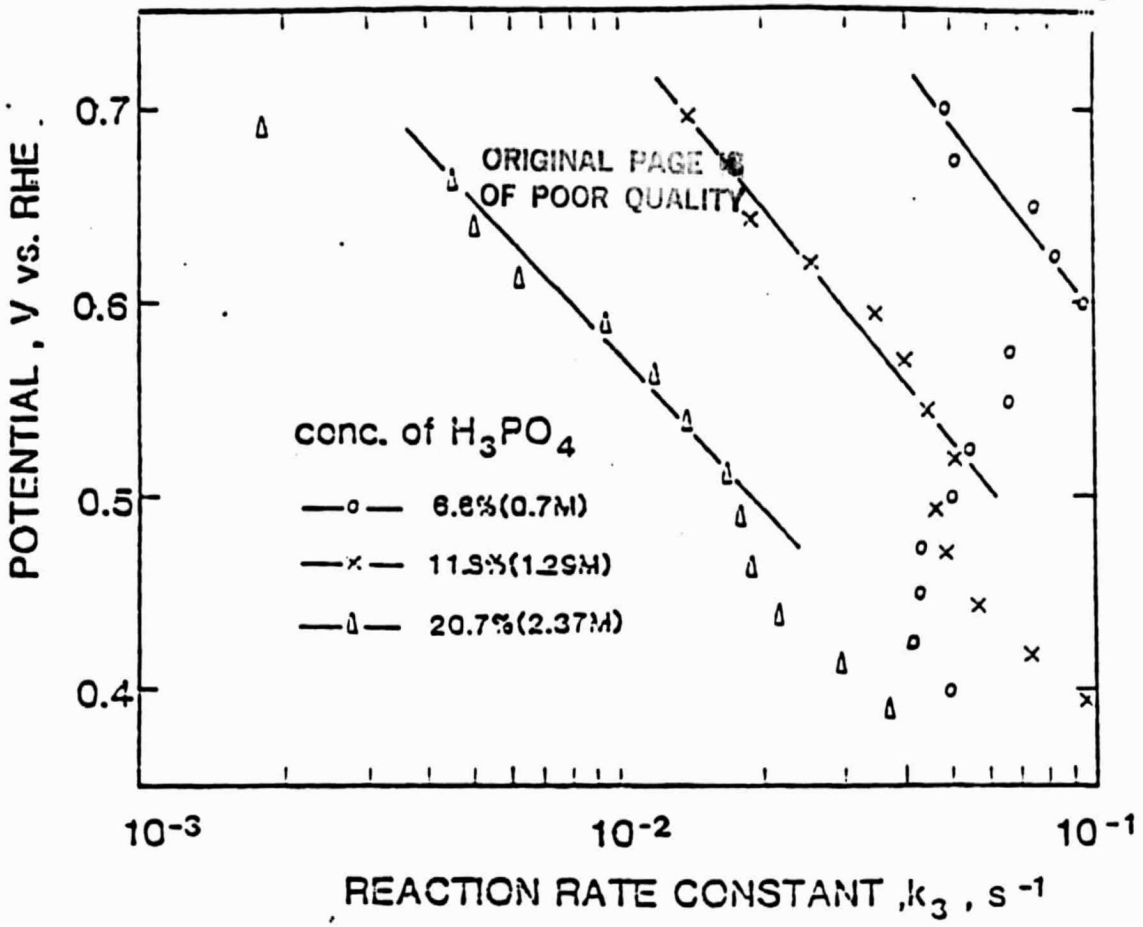

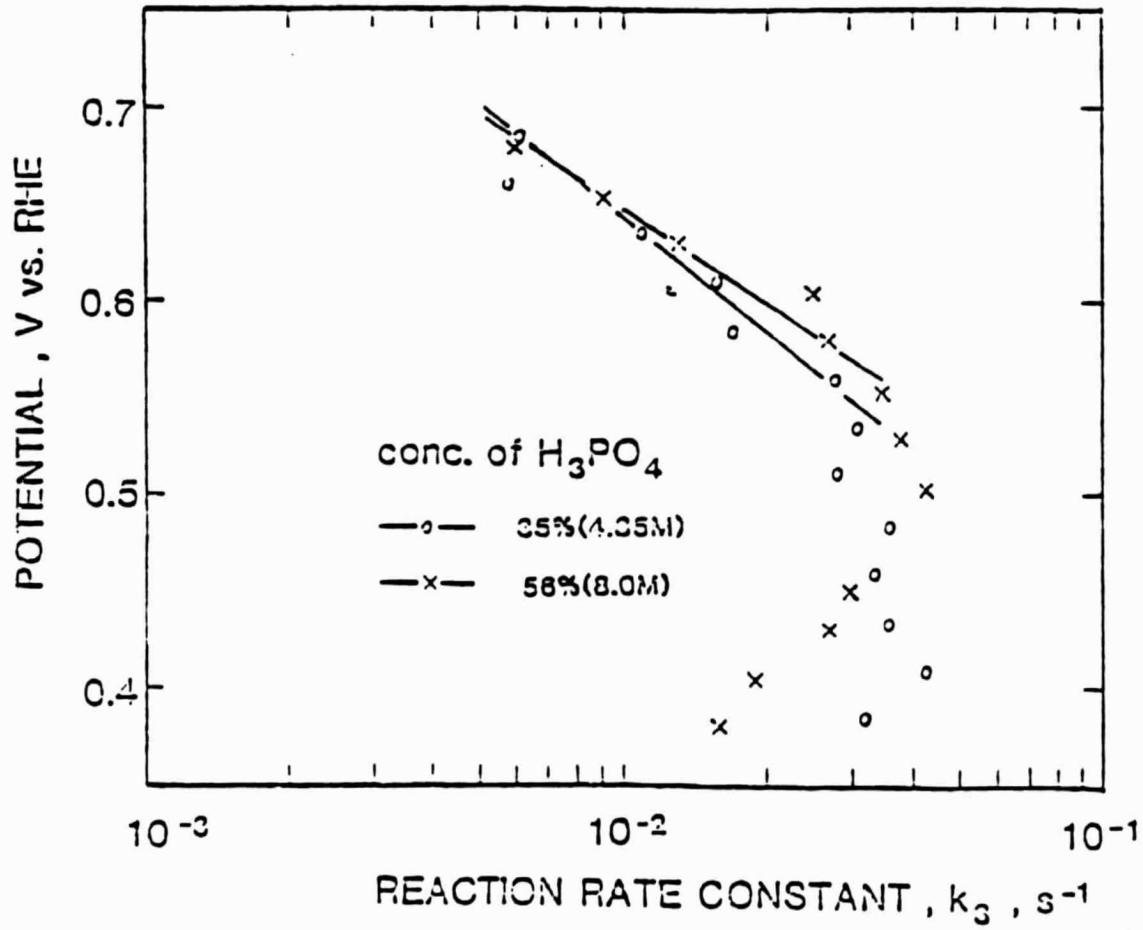

Fig. 10 Potential dependence of rate constant k_3 for oxygen reduction of Pt in H_3PO_4 in the concentration range 6.6 to 56 w/o at 25°C.

Conclusions

From the results of the rotating ring-disk experiment, the following conclusions may be reached for the oxygen reduction on pt in concentrated phosphoric acid solution: (i) In the potential range 0.8 to 0.6V, the slope of the mass transfer-corrected Tafel plots is equal to 120 mV/decade and is independent of concentration; (ii) The rate constants for k_1 and k_2 have the same potential dependence with the ratio of k_1/k_2 greater than 10.

2.4 ELECTRODE KINETICS OF OXYGEN REDUCTION ON PLATINUM IN TRIFLUOROMETHANESULFONIC ACID (TFMSA)

Trifluoromethanesulfonic acid (TFMSA, CF_3SO_3H) and its homologues of higher molecular weight are considered alternatives to phosphoric acid as acid electrolytes for fuel cell. The reaction rate of oxygen reduction at platinum in TFMSA is about two order of magnitude higher than that in phosphoric acid (23). Although there have been some investigations of oxygen reduction on platinum in aqueous TFMSA and in TFMSA monohydrate on smooth and porous electrode (23), its kinetics in this electrolyte is not yet fully understood. The purpose of this study is to investigate the kinetics of oxygen reduction at smooth platinum in aqueous TFMSA (0.05 ~ 6.0M) and in a mixed acid containing 1.0M TFMSA and 0.003 ~ 0.1M phosphoric acid.

Effects of Surface Oxide at Platinum on the Kinetics of Oxygen Reduction in TFMSA

During the rotating ring-disk experiment, when the electrode potential is scanned from 1.0 to 0.3 V vs. RHE, the surface of the platinum electrode is first covered with a layer of oxide and then gradually reduced to bare platinum at the end of the scan. Conversely when the electrode potential is scanned from 0.3 to 1.0 V vs. RHE, the electrode starts with an oxide-free surface and then the oxide is gradually formed at the potentials above 0.8 V vs. RHE.

The influence of the surface oxide on the kinetics of oxygen reduction at platinum in 0.05M TFMSA is shown in Fig. 11 (at ω = 900 rpm). The disk current (I_d) for oxygen reduction on the oxide-free surface (potential scanned from 0.3 to 1.0 V vs. RHE) was higher than that on the oxide-covered surface (potential scanned from 1.0 to 0.3 V vs. RHE). The maximum amount of hydrogen peroxide detected on the ring electrode (I_r) for the oxide-covered disk electrode was 400% higher than that for the oxide-free disk electrode.

Reaction Order with Respect to Oxygen for the Oxygen Reduction Reaction at Platinum in TFMSA

An attempt was made to determine the rate constants for oxygen reduction at platinum in TFMSA with the procedure of the theoretical analysis described in Section 2.2. Negative intercepts were observed for both the $I_{dl}/(I_{dl}-I_d)$ vs. $\omega^{-1/2}$ and I_d/I_r vs. $\omega^{-1/2}$ plots in all the TFMSA solutions (0.05 ~ 6.0M) as well as in 1.0M TFMSA solution with phosphoric acid additives (0.003 ~ 6.0M). One possible explanation is that the reaction order with respect to oxygen in the TFMSA medium is not unity. According to the following equation (24):

$$\log I_d = \log I_k + m \log (1 - I_d/I_{dl}) \qquad (4)$$

a plot of log I_d vs. log $(1 - I_d/I_{dl})$ should be linear with a slope equal to the reaction order of oxygen, m. A typical plot of log I_d vs. log $(1 - I_d/I_{dl})$ in 0.05M TFMSA is presented in Fig. 12. The slopes of the straight lines reveal a fractional reaction order. In the concentrations of TFMSA investigated, the reaction order of oxygen were between 0.4 and 0.5. In the mixtures of 1.0M TFMSA and 0.003 ~ 0.1M phosphoric acid, the reaction order of oxygen increased from 0.5 as the concentration of phosphoric acid increased.

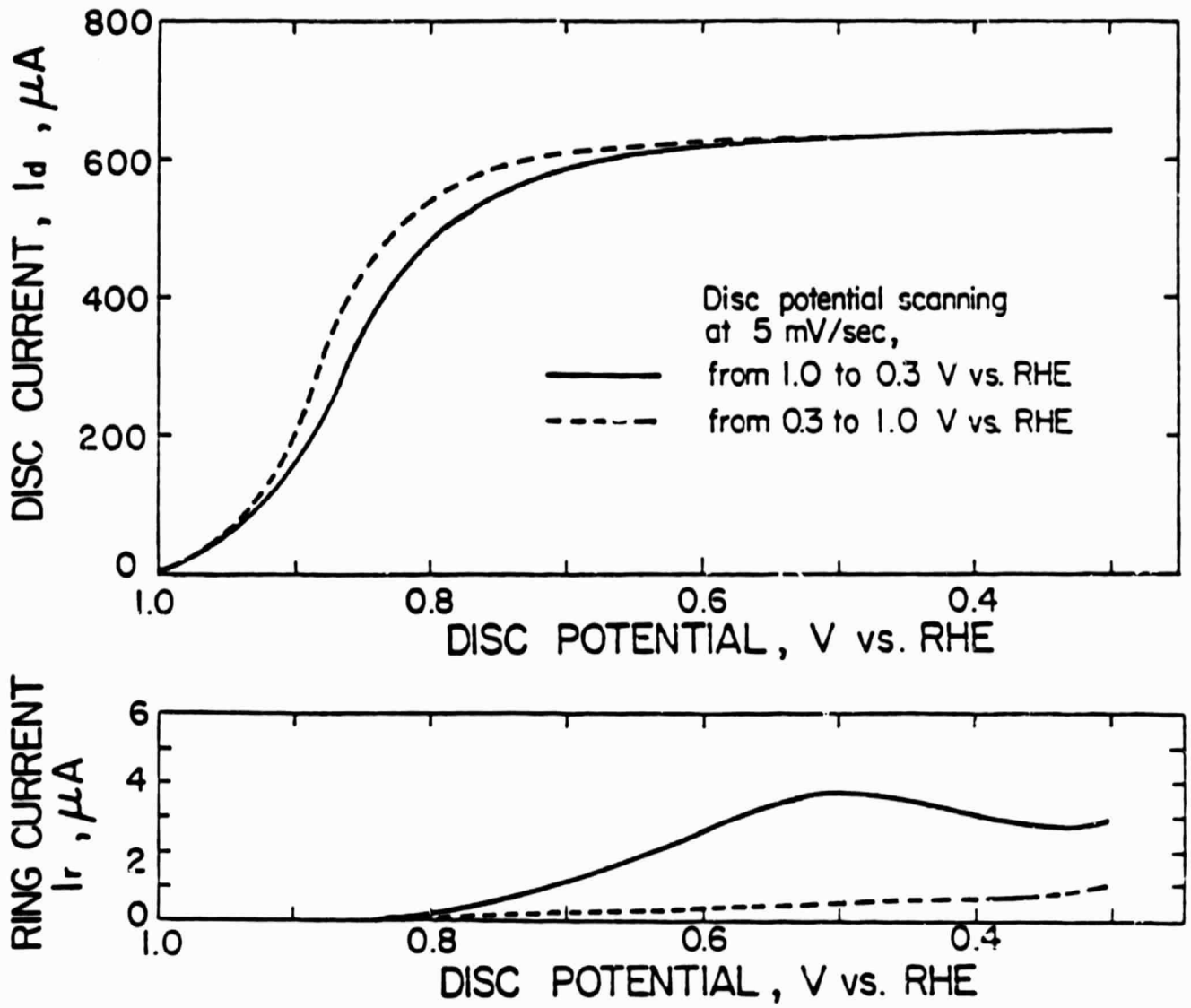

Fig. 11 The rotating ring-disc electrode data at ω = 900 rpm for oxygen reduction at Pt in 0.05 M TFMSA.

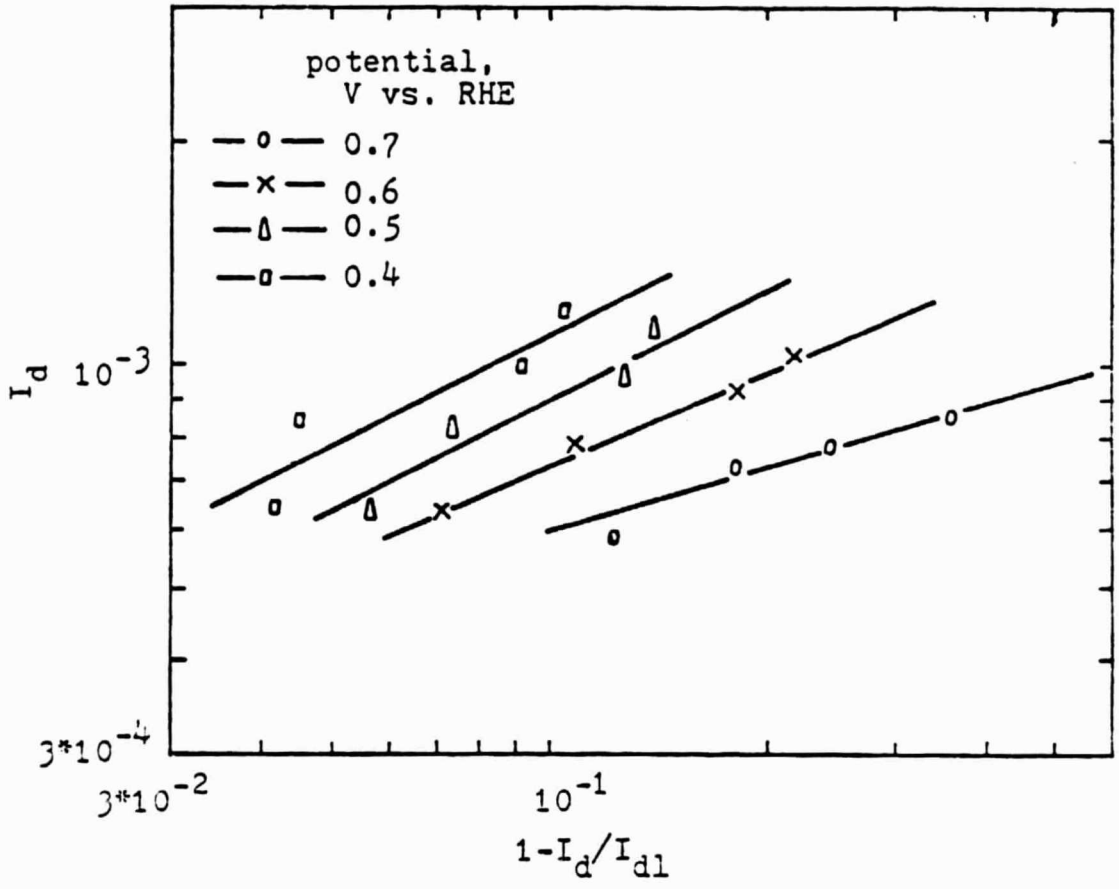

Fig. 12 Plot of log I_d vs. log$(1 - I_d/I_{dl})$. Data were obtained from the rotating ring-disk electrode experiments for oxygen reduction at Pt in 0.05 M TFMSA.

Mechanism of Oxygen Reduction at Platinum in TFMSA

For the reaction order of oxygen not equal to one, the mass transfer corrected Tafel equation is:

$$E = \frac{2.3RT}{\alpha F} \log I_o - \frac{2.3RT}{\alpha F} \log I_d \left(\frac{I_{dl}}{I_{dl} - I_d}\right)^m \qquad (5)$$

The plot of E vs. $\log I_d[I_{dl}/(I_{dl}-I_d)]^m$ should be independent of ω, if m is chosen properly. The plots with m=0.5 for oxygen reduction at platinum in TFMSA and in 1M TFMSA containing three concentrations of phosphoric acid are shown in Fig. 13 and 14, respectively. These plots are independent of ω. At a given potential, the reduction current decreased as the concentration of TFMSA of of phosphoric acid increased. The decrease in the oxygen reduction current in concentrated TFMSA is probably due to a lower oxygen solubility and/or higher anion adsorption. The decrease in the oxygen reduction current with the addition of phosphoric acid is due to the electrochemical active sites being blocked by the adsorption of phosphate ions.

Based on the proposed mechanism (21,25), the reaction order of one-half with respect to oxygen can be explained by considering a fast dissociation step (large k_1 and k_2 in Fig. 15) and that step 3 is rate determining (small k_3). By assuming that the adsorption of oxygen is under Langmuir condition, the disk current can be expressed by :

$$I_d = K[H^+][O_2]^{1/2} \exp\left[-\frac{\alpha F}{RT} E\right] \qquad (6)$$

In the above equation I_d is proportional to $[O_2]^{1/2}$.

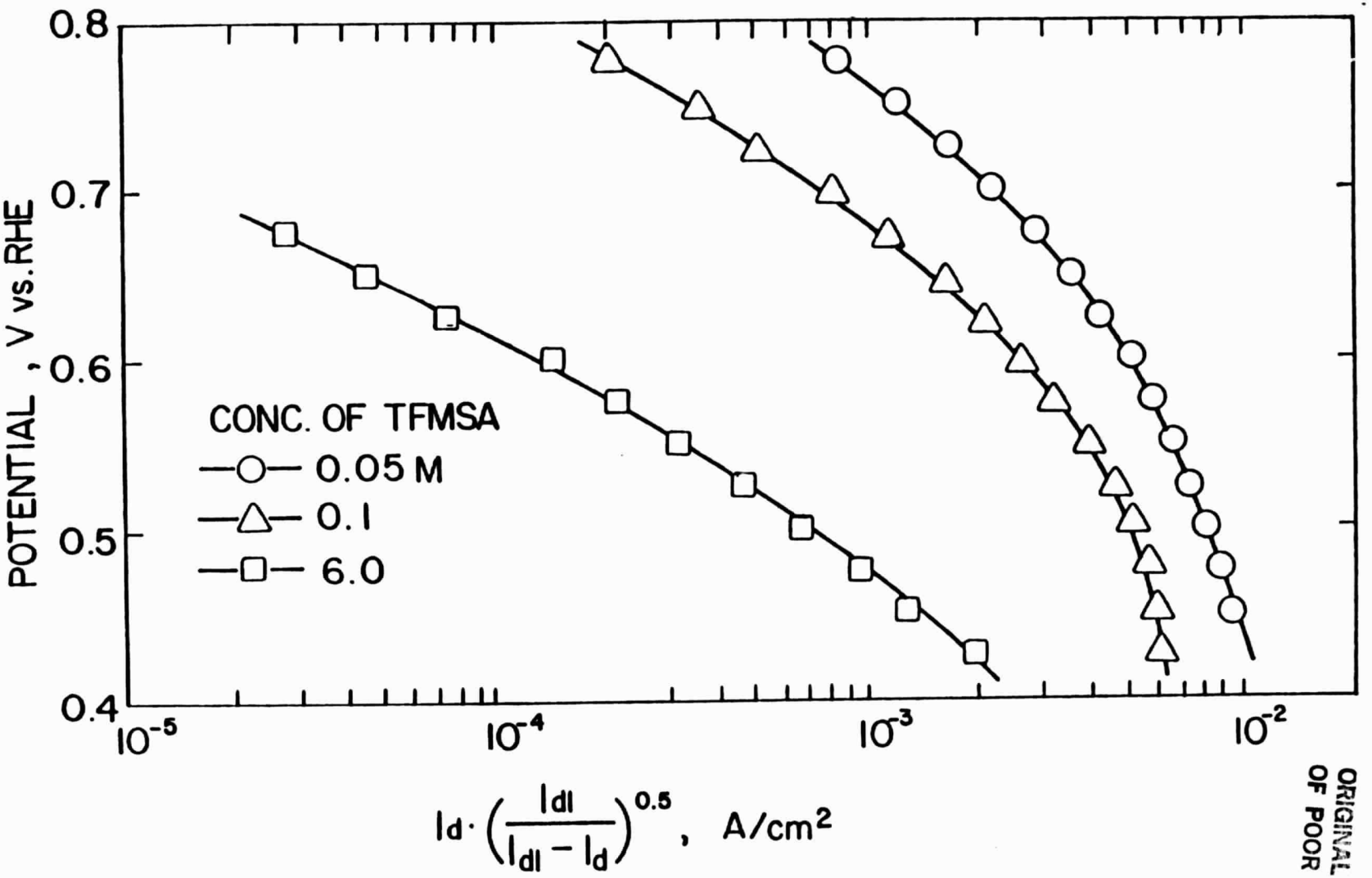

Fig. 13 The plot of potential against log $I_d[I_{dl}/(I_{dl} - I_d)]^{1/2}$ for oxygen reduction at Pt in different concentrations of TFMSA. This plot is independent of ω over the range of (400-3600 rpm).

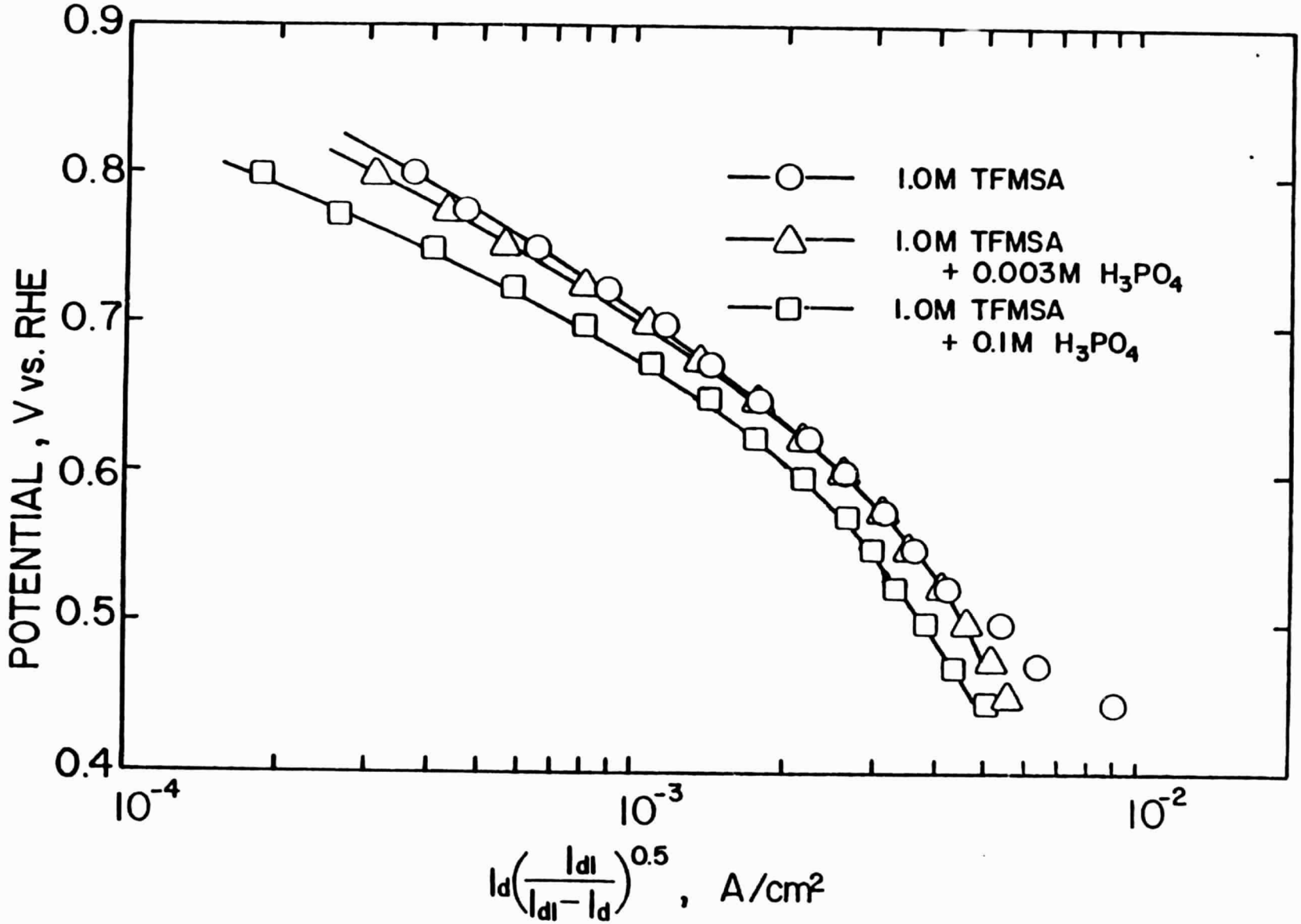

Fig. 14 The plot of potential against log $I_d[I_{d1}/(I_{d1}-I_{d1})]^{1/2}$ for oxygen reduction at Pt in 1.0 M TFMSA with the additives of H_3PO_4. This plot is independent of ω over the range of (400-3600 rpm).

Possible Mechanism of Oxygen Reduction at Pt in TFMSA : Under Langmuir adsorption condition , $\theta \neq \theta(E)$

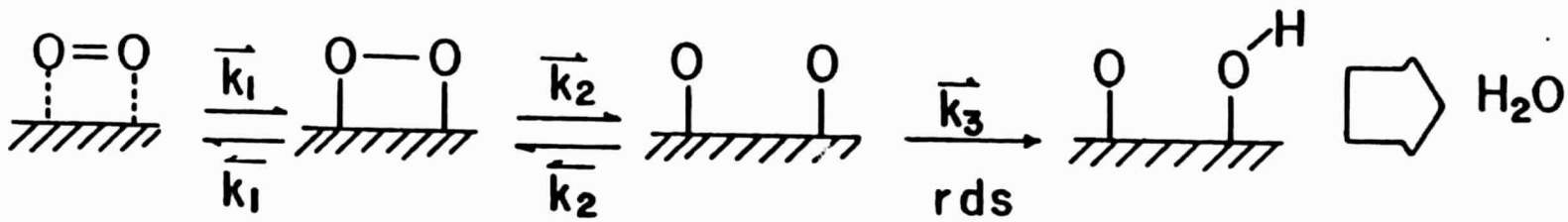

Fig. 15 Possible Mechanism of Oxygen Reduction at Pt in TFMSA: Under Langmuir adsorption condition, $\theta \neq \theta(E)$

Conclusions

From the rotating ring-disk electrode experimental data of oxygen reduction at platinum in TFMSA, it can be concluded that (i) a lower oxygen reduction current and a larger amount of hydrogen peroxide were observed for the oxide-covered platinum surface as compared to the oxide-free surface; (ii) a half reaction order with respect to the oxygen concentration was obtained; (iii) on the basis of the present experimental results, a reaction mechanism involving the fast dissociative adsorption of oxygen followed by the slow first charge transfer step was proposed for oxygen reduction at platinum in TFMSA.

III. TRANSPORT PROPERTIES OF PHOSPHORIC ACID ELECTROLYTE

3.1 LITERATURE REVIEW

The transport properties of the phosphoric acid electrolyte are needed to study the electrode kinetics of oxygen reduction reaction and to optimize the fuel cell performance. Among these, the electric conductivity, viscosity, diffusivity and solubility of oxygen in the electrolyte are the most important properties.

Electric Conductivity

Several sets of conductivity data for phosphoric acid at various concentrations and temperatures are available in the literature. Some of the early data are presented in the Monsanto Technical Bulletin (26), which also includes unpublished data of Helmer et al. (27). Increased attention has been shown recently in obtaining conductivity at high concentrations and temperatures. (28-34); such an emphasis has left a gap in the literature on the data of conductivity and other properties. Table 1 summarize the available data of electric conductivity (35). It is evident that over the concentrations range of 0-85% phosphoric acid, there are no data available for temperatures greater than 25°C. Also, for the concentrations range of 85 - 100% H_3PO_4, no data are available for temperatures greater than 150°C. A more complete set of data is needed.

It is suggested that for dilute phosphoric acid concentrations, the major contribution to conductivity must come from the Stokesian ion transport, whereas in more concentrated solutions the major contribution to conductance comes from proton switch (chain type) mechanism. The existence of proton switch mechanism in water is well established. There are evidences which support the existence of proton switch mechanism in H_3PO_4.

Greenwood and Thompson (32) considered the self dissociation of anhydrous phosphoric acid according to the equilibria:

$$2\ H_3PO_4 \rightleftharpoons H_4PO_4^+ + H_2PO_4^- \quad \text{[fast]} \tag{7}$$

$$2\ H_3PO_4 \rightleftharpoons H_3O^+ + H_3P_2O_7^- \quad \text{[slow]} \tag{8}$$

The first equilibrium is labelled fast because the conductivity of freshly melted phosphoric acid is high ($7.68 \times 10^{-2}\ \Omega^{-1}\ cm^{-1}$). Since the ionic dissociation is very small (as low as 4.5% for the hemi-hydrate), and the viscosity is high for H_3PO_4, the observed high conductivity can not be explained in terms of Stokesian diffusion. This means that other type of transport mechanism must have a significant contribution to the conductivity. Gileadi (36) has represented the switch mechanism for $H_2PO_4^-$ migration as shown in Fig. 16, where phosphoric acid molecules and phosphate anions are associated by hydrogen bonds. Under an electric field, the proton tends to migrate. According to Gileadi, the switching of protons can be accomplished by either rotating or the rearrangement of the internal bonds as shown in the figure. The latter being more favorable considering the large energy that would be required to reorient the associated phosphoric acid molecules. The same view point of a hydrogen bonded network has also been proposed by Akiyama et al. (34). To support their hypothesis, these authors calculated the molar conductance of concentrated phosphoric acid assuming both water and phosphoric acid contribute to conduction. The calculated molar conductance was constant between 60 and 76% P_2O_5 content. Further evidence for proton migration comes from the work of Greenwood and Thompson (32). They hypothesize that if a certain H-bonding structure is responsible for proton migration, then the conductivity would decrease if the probability of H-bond formation is reduced. To prove this, these authors prepared the co-ordinated complex of H_3PO_4 and BF_3.

Table 1. Specific Conductivity of Phosphoric Acid as a Function of Concentration and Temperature. Compiled from References 37, 7, 8, 9.

unit: $ohm^{-1} \cdot cm^{-1}$

0°-45.0°C

Temp °C	0°	18°	25°	29.3	30°	35	40°	45.0
wt% H_3PO_4								
1			0.0102					
2			.0175					
3			.0226					
4			.0281					
5	0.0409		.0334					
10	.0615	0.0566	.0617					
15	.0772	.0850	.0918					
20	.0934	.1129	.1236					
25	.1096	.1402	.1553					
30	.1259	.1654	.1836					
35	.1415	.1858	.2068					
40	.1472	.2010	.2236					
45	.1488	.2087	.2336					
50	.1427	.2073	.2324					
55	.1317	.1978	.2263					
60	.1195	.1833	.2117					
65	.1052	.1650	.1905					
70	.0844	.1436	.1656					
75	.0608	.1209	.1373					
80	.0460	.0979	.1118					
85	.0348	.0780	.0907					
85.10	.							
85.79	.		.0888		0.102		0.134	
88.47	.		.0801		.0928		.122	
88.68								
89.10								
90	.0245	.	.0673	0.0850				
90.45								
90.54			.0734		.0858		.114	
91.42								
92.75								
93.73			.0641		.0756		.102	
95	.0184		.0612	.0696				
96.97								
97.07			.0535		.0639		.0870	
97.96								
98.93								
99.57								
99.75			.0447		.0534		.0740	
99.72								
100			.04675		.05589	.06598	.07680	.08836
101.63			.0355		.0432		.0606	
104.43			.0210		.0262		.0389	
106.77			.0115		.0148		.0234	
110.49			.00336		.00471		.00865	
112.58			.00175		.00256		.00495	
115.66			.000860		.00125		.00245	
118.16			.000183		.000282		.000597	

Table 1. SPECIFIC CONDUCTIVITY (continued)

unit: $ohm^{-1}\ cm^{-1}$

	50.0°-170.42°								
Temp °C	50°	55°	60.0	65.0	130.00	140.12	150.25	160.92	170.42
wt% H_3PO_4									
3									
1									
2									
3									
4									
5									
10									
15									
20									
25									
30									
35									
40									
45									
50									
55									
60									
65									
70									
75									
80									
85									
85.10					0.4904	0.5299	0.5685		
85.79	0.167		0.202						
88.47	.154		.189						
88.68									
89.10					.4747	.5169	.5589	0.6033	
90									
90.45					.4702	.5133	.5568	.6020	0.6411
90.54	.146		.180						
91.42					.4665	.5098	.5536	.5996	.6397
92.75					.4606	.5055	.5495	.5960	.6384
93.73	.131		.165						
95									
96.97					.4369	.4816	.5280	.5763	.6184
97.07	.115		.145						
97.96					.4274	.4717	.5178	.5664	.6082
98.93					.4137	.4578	.5029	.5516	.5936
99.57					.4019	.4461	.4904	.5386	.5819
99.75	.0975		.124						
99.72					.3986	.4421	.4872	.5347	.5774
100	.1013	0.1138	.1270	0.1406					
101.63	.0814		.106						
104.43	.0550		.0744						
106.77	.0346		.0490						
110.49	.0141		.0220						
112.58	.00855		.0137						
115.66	.00429		.00699						
118.16	.00108		.00183						

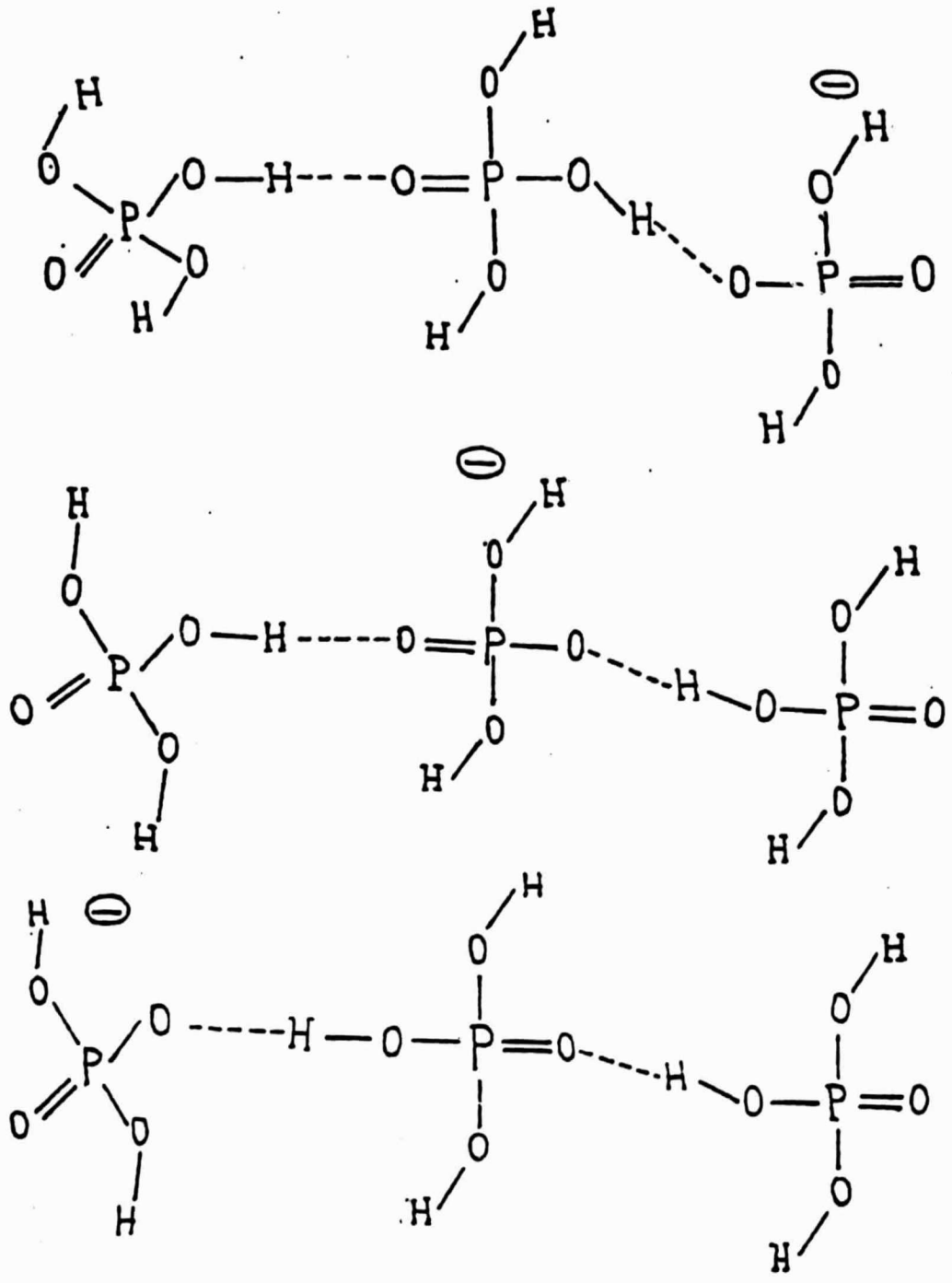

Fig. 16 A schematic diagram of the hopping mechanism in H_3PO_4

The viscosity and electric conductivity of these complexes were markedly different from those of H_3PO_4. These results could be explained only by the presence of a hydrogen bonding network in H_3PO_4. Munson (38) studies the effect of various ionic solutes on the conduction of H_3PO_4 and came to the same conclusions as those of Greenwood and Thompson.

Kinetic Viscosity

The existing literature data on the kinematic viscosity of phosphoric acid are summarized in Table 3-2. The accuracy of the data is estimated to be ± 15%. Saji (40) reported viscosity data for concentrated phosphoric acids which deviated from that reported in Table 2; the difference occurs red because the acid was dehydrated by heating and contains higher proportions of Poly-acids. The effect of various impurities like Al, Fe, k, Ca, Mg on the viscosity of phosphoric acid has been discussed by Cate and Deming (41), and by Dahlgren (42). The cations increase the viscosity, while anions have negligible effect. The effects are negligible at the concentration below 0.1% by weight of the impurity; the magnitude of the effect is also dependent on the concentration of the phosphoric acid.

As seen in Table 2, there are some gaps in the kinematic viscosity data. For 0-85% H_3PO_4, no data are available for temperature greater than 180°C. The kinematic viscosity data have been correlated by Kondrachenko et al. (43-44) with a polynomial equation for the concentration range 90-103% H_3PO_4 at temperature from 20 to 90°C.

Table 2 KINEMATIC VISCOSITY OF PHOSPHORIC ACID SOLUTIONS

% H_3PO_4	Temperature, °C.																	
	20	25	30	40	50	60	70	80	90	100	110	120	130	140	150	160	170	180
0	1.0	0.90	0.85	0.74	0.66	0.61	0.42	0.37	0.33	0.30								
5	1.1	0.99	0.89	0.74	0.63	0.54	0.47	0.42	0.37	0.33								
10	1.2	1.1	0.95	0.83	0.71	0.61	0.54	0.47	0.42	0.38								
15	1.4	1.2	1.1	0.94	0.81	0.69	0.61	0.53	0.47	0.43								
20	1.6	1.4	1.3	1.1	0.92	0.78	0.69	0.61	0.54	0.49								
25	1.8	1.6	1.5	1.2	1.0	0.89	0.79	0.69	0.61	0.55								
30	2.2	1.9	1.7	1.4	1.2	1.0	0.90	0.79	0.70	0.62								
35	2.6	2.2	2.0	1.6	1.3	1.1	1.0	0.90	0.79	0.71								
40	3.0	2.6	2.3	1.9	1.5	1.3	1.2	1.0	0.90	0.81								
45	3.6	3.1	2.7	2.2	1.8	1.5	1.3	1.2	1.0	0.92								
50	4.3	3.7	3.3	2.6	2.1	1.8	1.6	1.4	1.2	1.1								
55	5.3	4.5	4.0	3.2	2.5	2.1	1.9	1.6	1.4	1.2	1.1							
60	6.6	5.6	5.0	3.9	3.1	2.5	2.2	1.9	1.7	1.4	1.3							
65	8.4	7.2	6.2	4.9	3.8	3.1	2.6	2.3	2.0	1.7	1.5	1.4						
70	11	9.2	7.8	6.1	4.7	3.8	3.2	2.7	2.4	2.0	1.8	1.6						
75	15	12	10	7.5	5.9	4.8	3.9	3.3	2.8	2.4	2.1	1.9	1.7					
80	20	17	14	10	7.6	6.2	4.9	4.1	3.4	3.0	2.6	2.3	2.0	1.8				
85	28	23	19	14	10	8.1	6.3	5.1	4.2	3.5	3.2	2.8	2.4	2.2	1.9			
90	41	34	27	19	14	11	8.3	6.5	5.3	4.2	3.6	3.1	2.8	2.4	2.1			
95	68	55	42	30	20	15	12	8.7	7.3	6.2	5.2	4.4	3.8	3.3	3.0	2.6	2.3	2.1
100	140	100	81	53	36	25	19	14	11	9.2	7.7	6.3	5.2	4.5	4.1	3.5	3.2	2.9
105	600	440	330	173	110	70	50	33	25	19	15	12	9.6	8.0	7.1	6.0	5.2	4.5
110		2200	1600	810	410	270	170	100	67	50	38	29	22	18	15	13	10	8.2
115						1500	1000	600	380	250	190	120	91	68	54	41	34	28
116								2000	1200	830	550	430	320	210	170	130	107	87

Viscosities expressed in centistokes

Diffusivity and Solubility of Oxygen in Phosphoric Acid Electrolyte

Oxygen solubility in concentrated phosphoric acid solution was first determined by Gubbins and Walker (45) using a gas chromatrographic method. Yatskovskii and Fedotov (46) measured the solubility and diffusivity of oxygen at 25°, 45° and 60°C as a function of the phosphoric acid concentration (up to 85% by weight) using an electrochemical method; in this method, a platinum wire was sealed into a capillary and oxygen diffused to the electrode through the open end of the capillary. Klinedinst et al. (47) extended the measurement from 85% to 96% acid concentrations. The authors used a diffusion current-time curve to a platinum wire electrode to determine the oxygen solubility and diffusivity.

There was reasonable agreement between the results of Gubbins et al. and those of Yatskovskii et al.; in both these investigations the solubility decreased with concentrations of the acid. The results of Klinedinst et al. were consistent with those of Gubbins and Walker at a given concentration and temperature, but the concentration dependence was exactly opposite to that observed by Gubbins. The activation energy for oxygen diffusivity reported by Klinedinst was also different from the value calculated by Yatskovskii et al. Unfortunately, a critical comparison of these results is not possible since Klinedinst did not carry out measurement for the concentrations lower than 85% at 25°C.

3-2 EXPERIMENTAL

In the present work, the electric conductivity and kinematic viscosity of phosphoric acid electrolyte have been measured over a range of concentrations from 7% to 100%, and the temperatures from 25° to 200°C.

Electric Conductivity

Electrical conductivity data were measured with an A.C. conductivity bridge and conductivity cell (Beckman). The cell constant of the conductivity cell was calibrated with standard 0.01 N KCl solution.

The specific conductivity of phosphoric acid was measured over a concentration range of 0-100% and a temperature range of 25-200°C. The electrolytes were made from stock 85% phosphoric acid (Fisher). For concentrations 0-85% acid, the different solutions were diluted from 85% H_3PO_4 with distilled water. For concentrations greater than 85%, the solutions were made by concentrating purified acid inside a vacuum oven. The solution was poured into a three arm round-bottom flask, and immersed in an oil bath. A reflux column was used to condense any vapor at high temperatures (greater than 100°C.) A thermometer was used to monitor the temperature of the solution for each concentration, the specific conductivity data for different temperatures were taken at a 10°C temperature increment.

Kinematic Viscosity

Kinematic viscosity data were measured with a Canon-Fenske viscometer made by Industrial Glass Co. The time constants of the vocometers were calibrated against water and glycerol solutions at different temperatures. The range of concentrations measured for kinematic viscosity was the same as that of specific conductivity. The temperature range was slightly different; it was from 25 to 180°C. The measurement was carried out in a constant temperature air oven.

3.3 RESULTS

Electric Conductivity

The specific conductivity of phosphoric acid solution has been measured over a concentration range of 6-100% (by weight) and a temperature range of 25-200°C. The data are presented in graphical form in Figs. 17-22.

Figure 17 is a plot of specific conductivity as a function of concentrations at 25, 100 and 170°C. For each temperature, the curve exhibits a maximum at a certain concentration; this maximum shifts toward higher concentration with increasing temperature. Figures 18-22 are the

semi-logarithmic plots of specific conductivity versus reciprocal of absolute temperature at different concentrations. Figure 18 is for concentration range of 0.05 to 2.37 M phosphoric acid. It is seen that conductivity increases with temperature and that straight lines can be drawn for the conductivity at the low concentrations. At higher concentrations, the Arrhenius type correlation does not hold. This can be seen in Figs. 19-22; for there concentrations, a second order polynomial fit of ln k vs. 1/T should give a better description of the experimental data.

Kinematic Viscosity

The kinematic viscosity of phosphoric acid was measured for the concentration range of 6-100% and the temperature range of 25-180^{o}C. The data are presented graphically in Figs. 23-27.

Figure 23 is a plot of kinematic viscosity as a function of concentrations at 25, 100, and 170^{o}C. The kinetic viscosity increases exponentially as the concentration increases. However, the increases becomes less drastic at high temperatures. The kinetic viscosity decreases with increasing temperature. Figures 24-27 are the semi-logarithmic plots of kinematic viscosity versus reciprocal temperatures at different concentrations. The kinematic data seem to obey the Arrhenius law at the concentration and temperature range investigated.

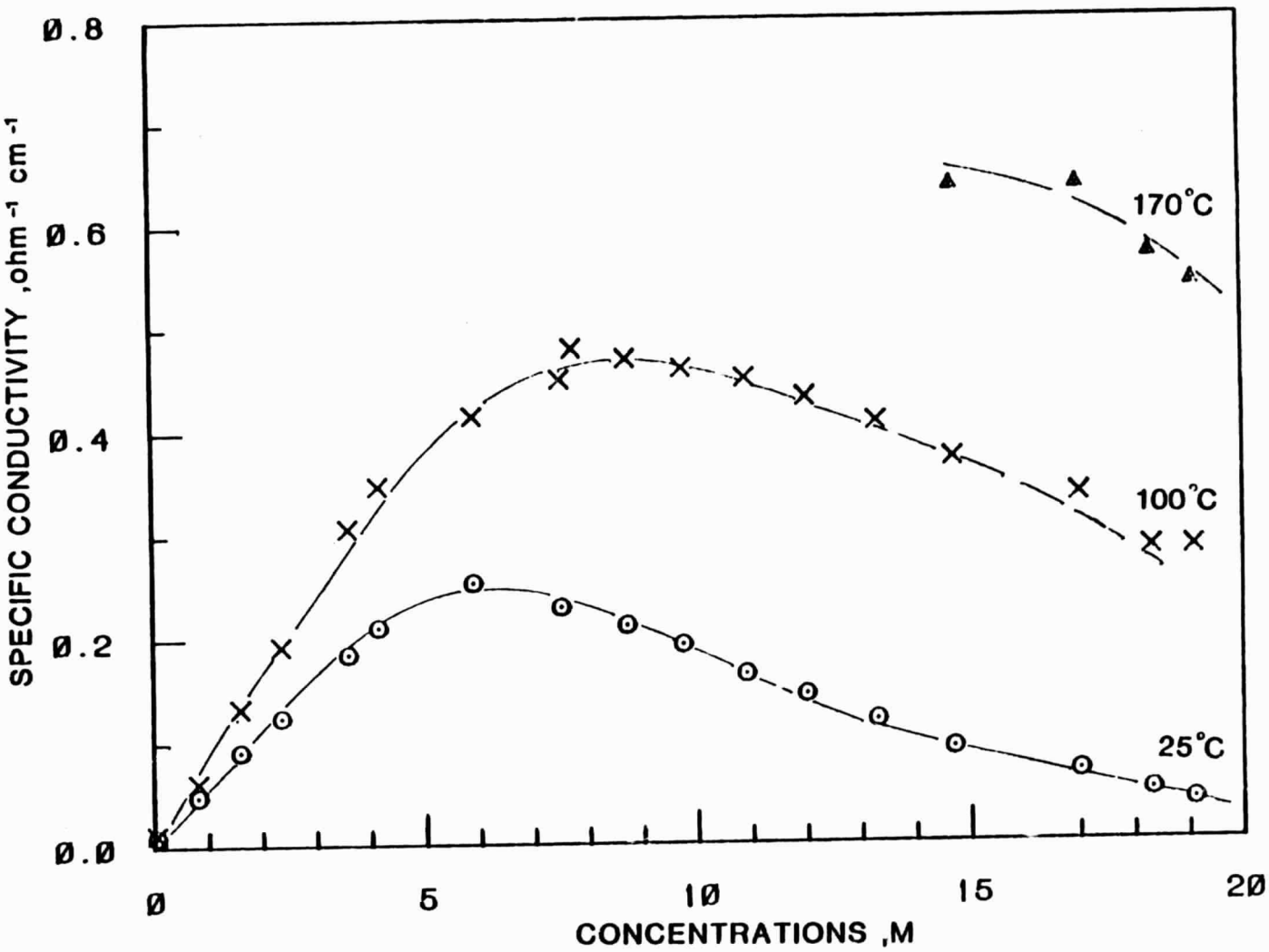

Figure 17 Effect of concentrations on conductivity at 25°, 100°, 170°C

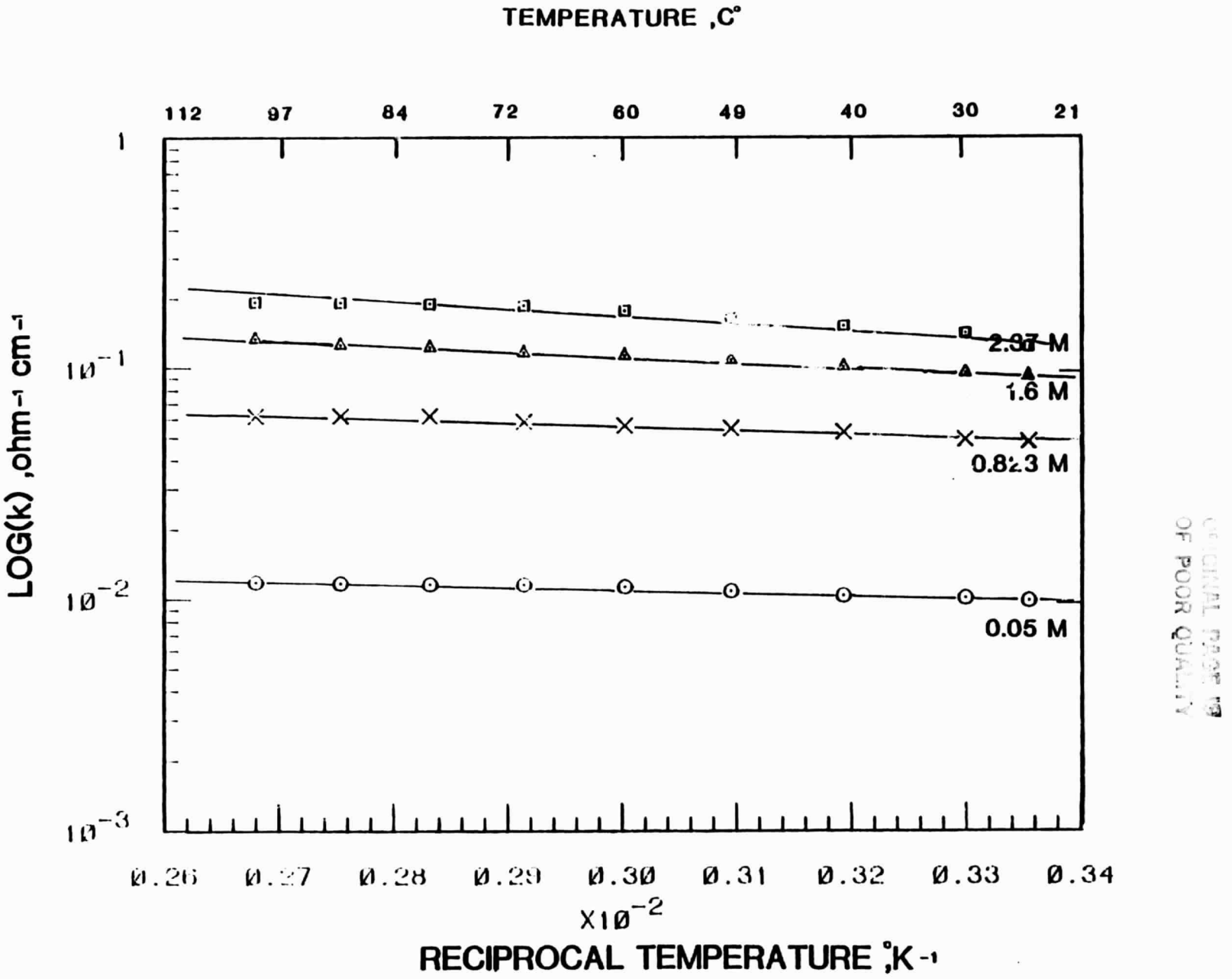

Figure 18 Plot of specific conductivity versus reciprocal temperatures at dilute concentrations

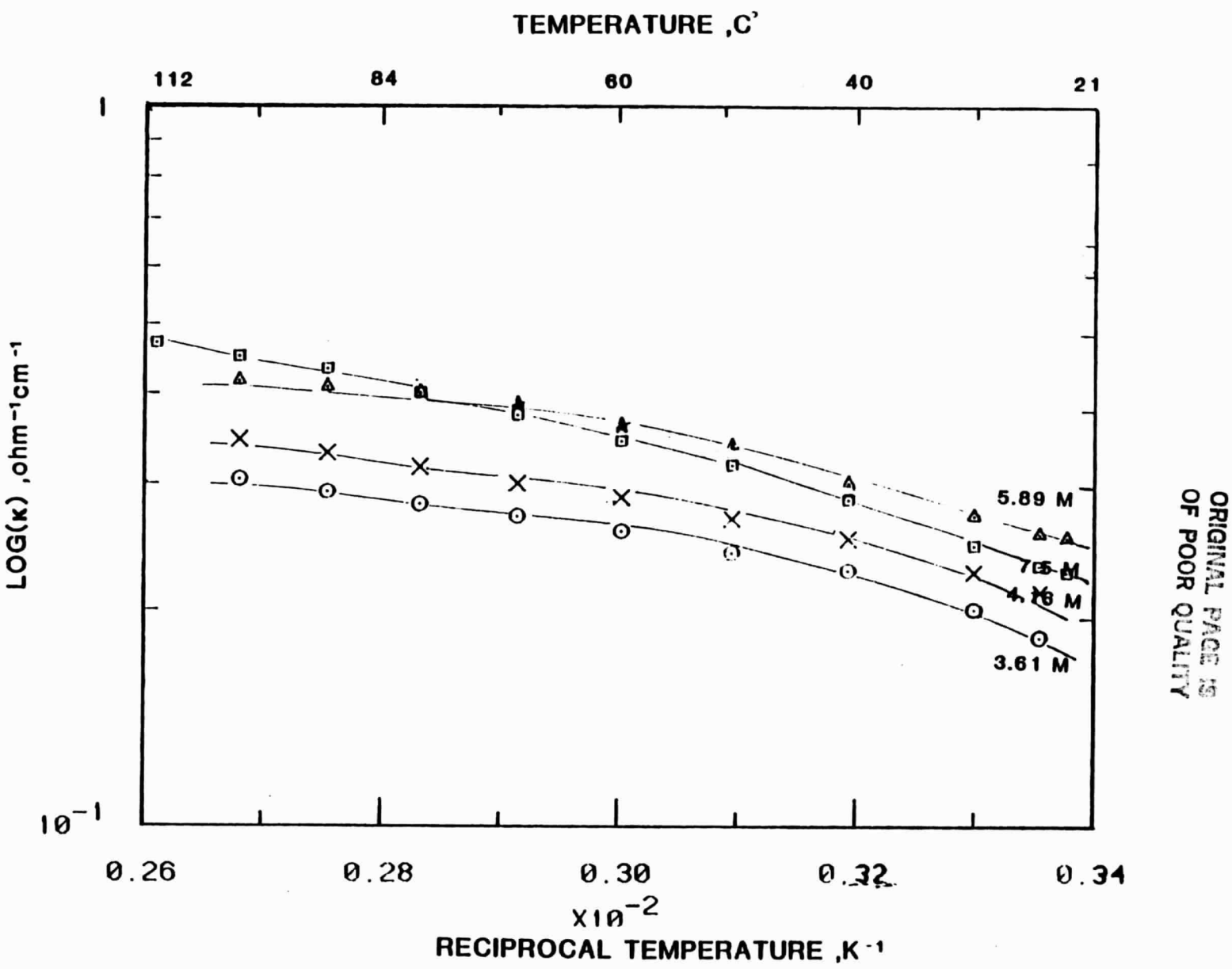

Figure 19 Plot of specific conductivity versus reciprocal temperatures at 3.6 to 6 M H_3PO_4

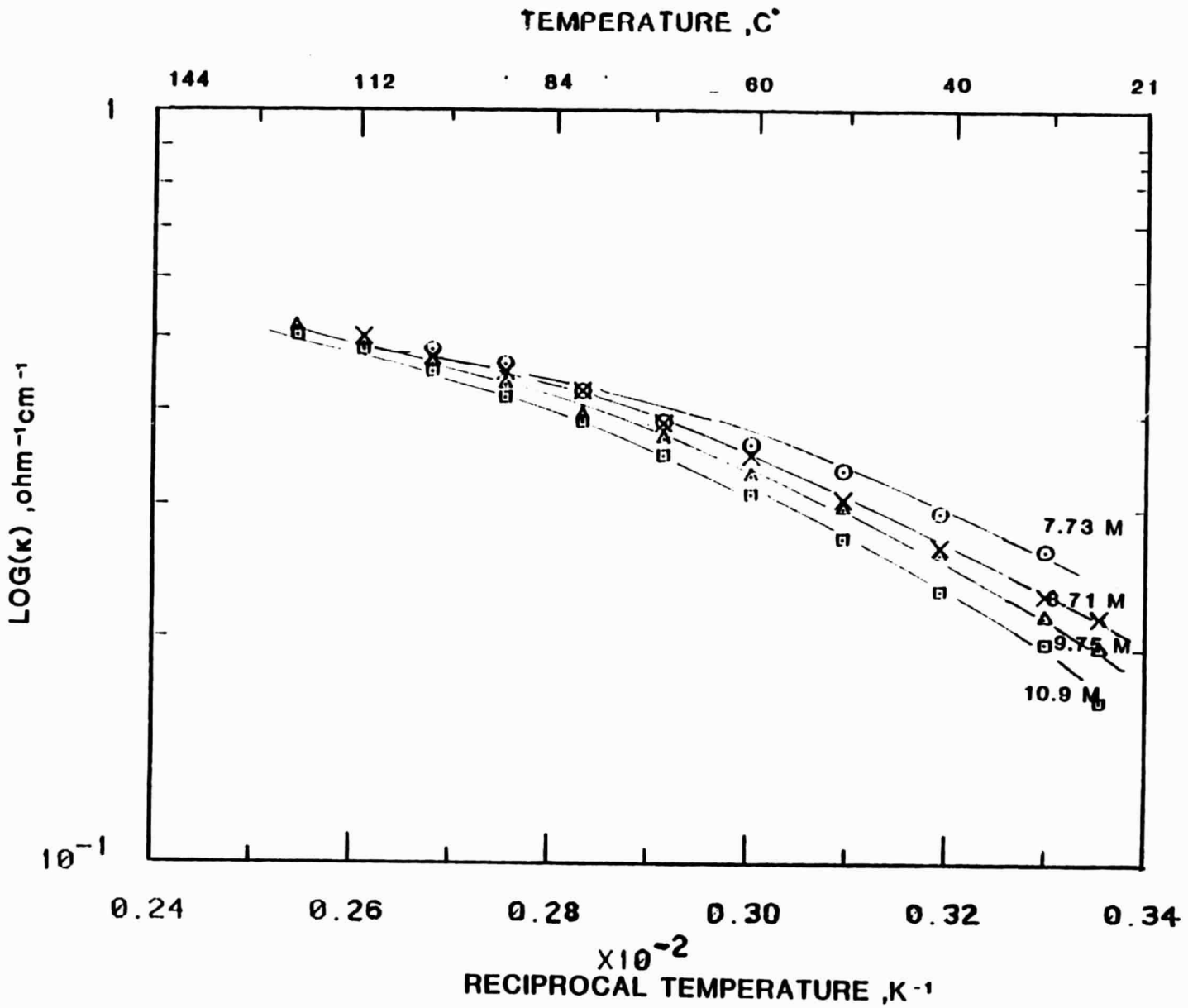

Figure 20 Plot of specific conducting versus reciprocal temperatures at 7.73 to 10.9 M H_3PO_4

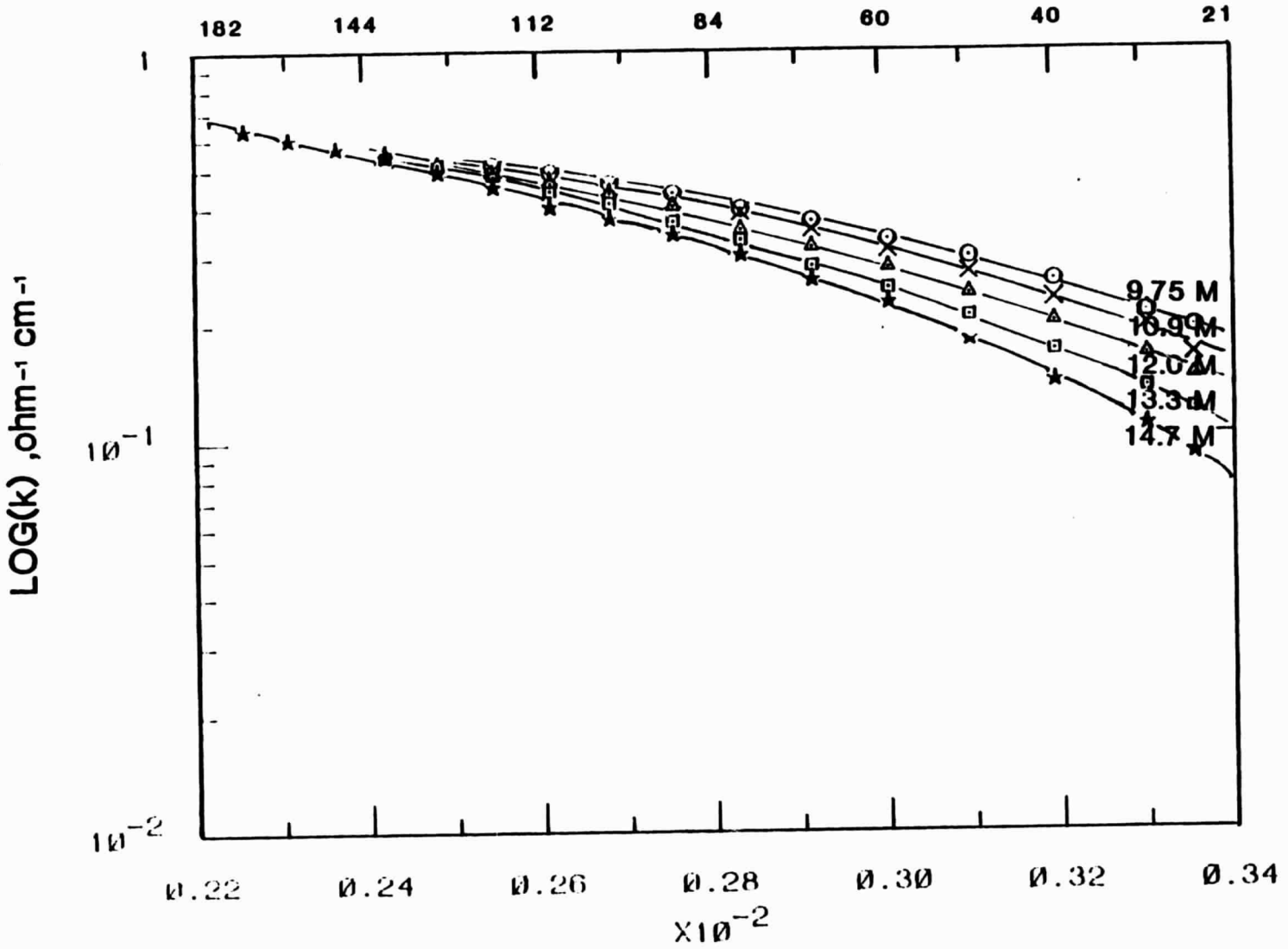

Figure 21 Plot of specific conductivity versus reciprocal temperature at 9.75 to 14.7 M H_3POP_4

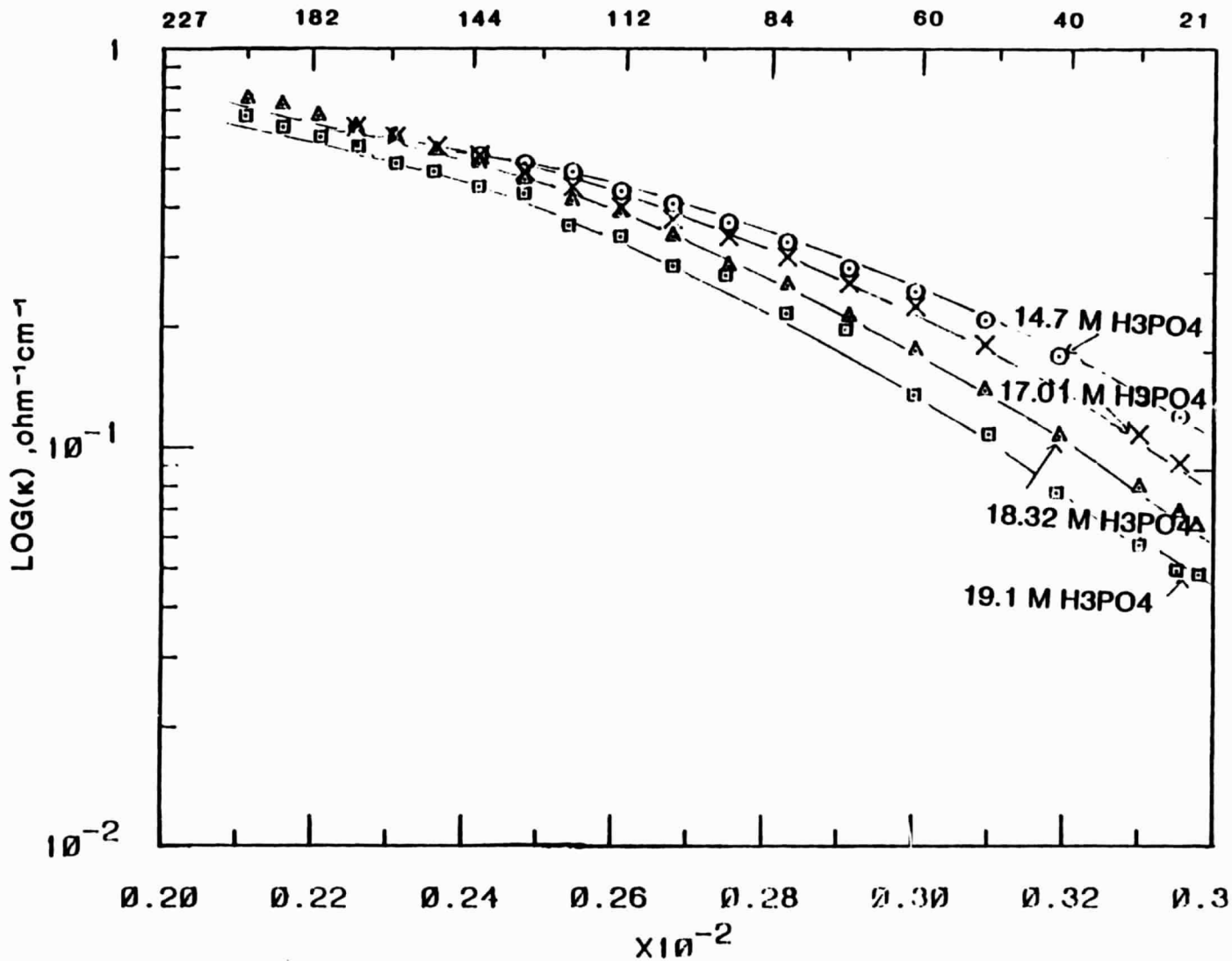

Figure 22 Plot of specific conductivity versus reciprocal temperature at concentrates H_3PO_4

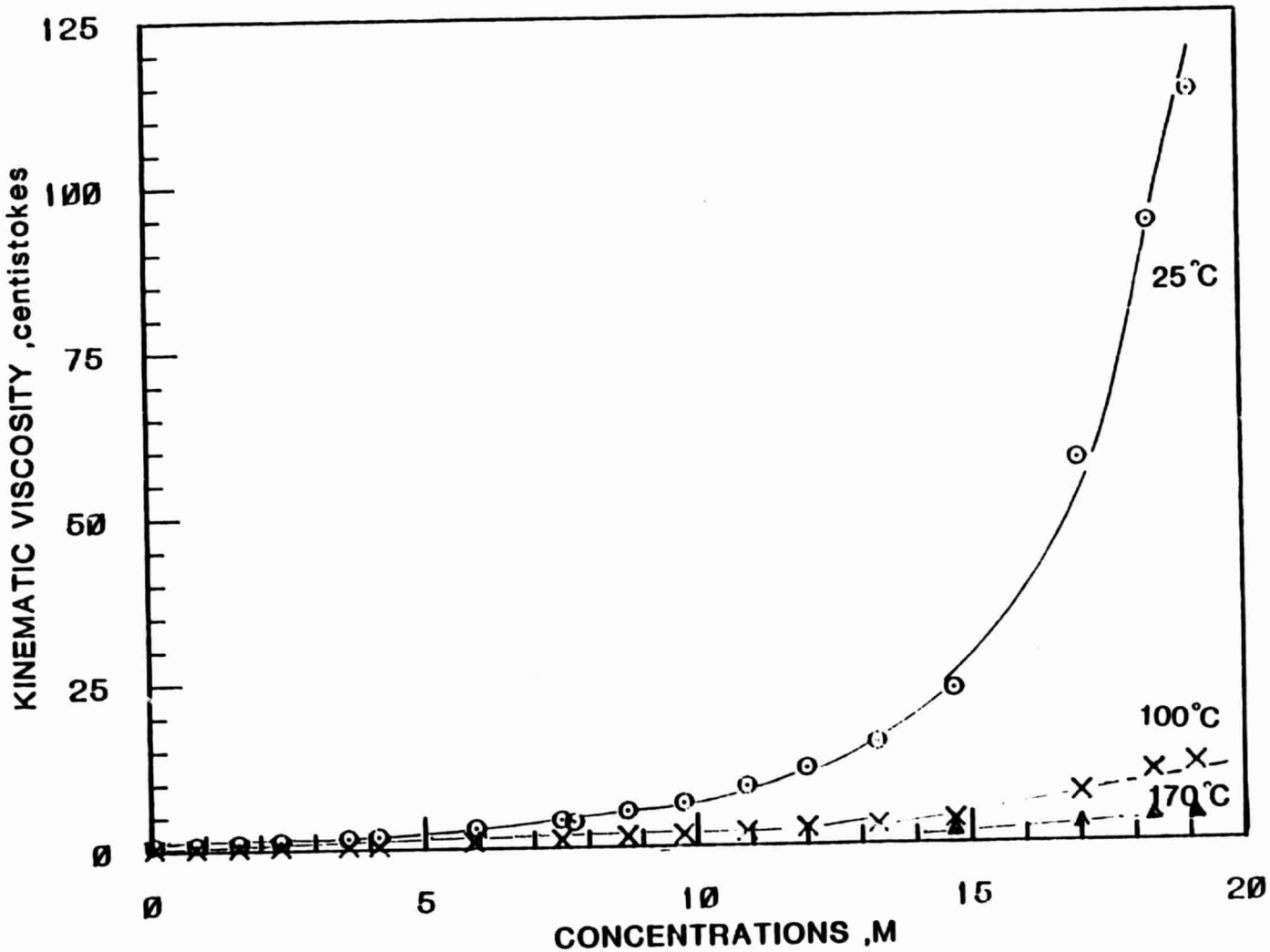

Figure 23 Effect of concentrations on kinematic viscosity at different temperatures

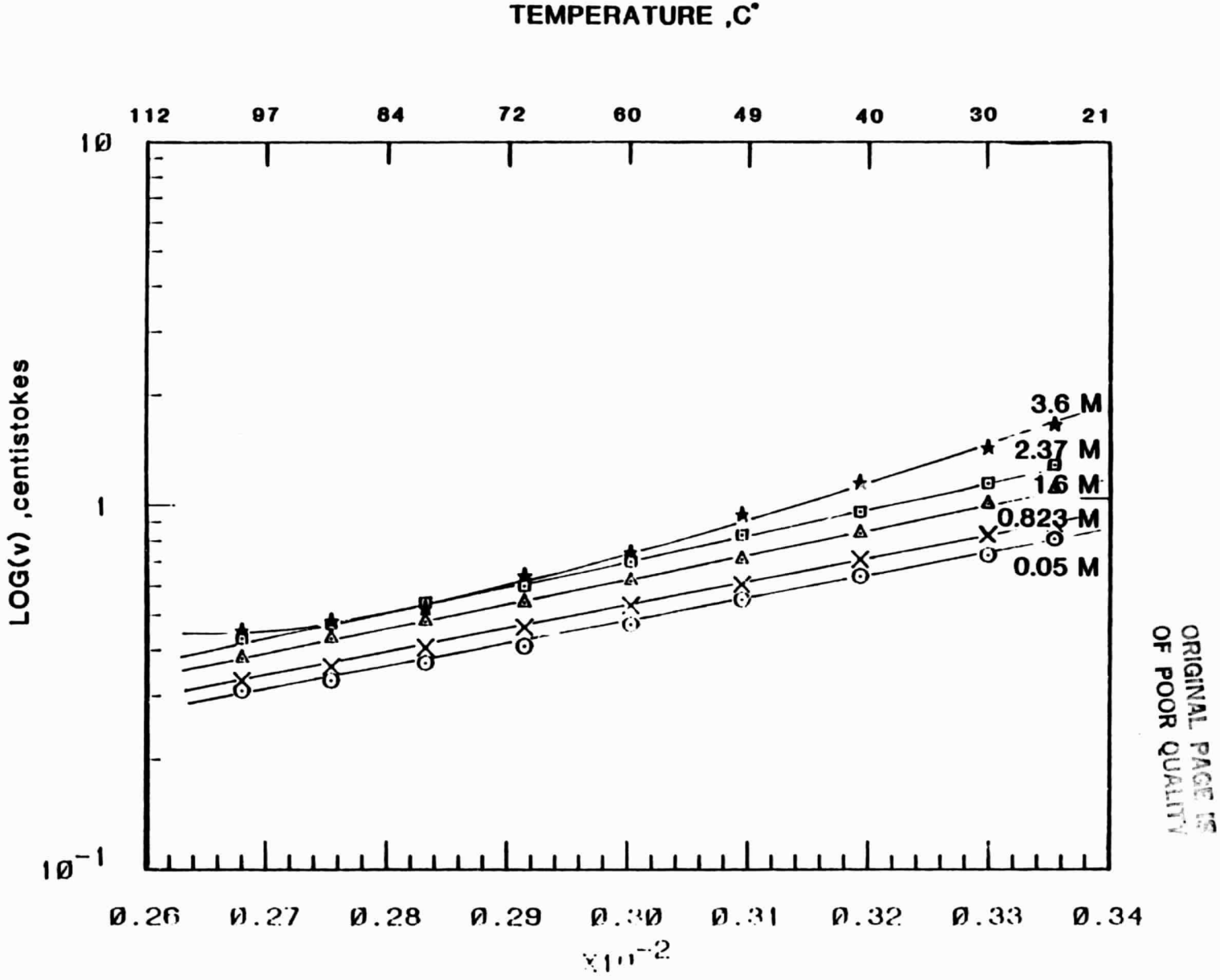

Figure 24 Plot of kinematic viscosity versus reciprocal temperature at dilute concentrations

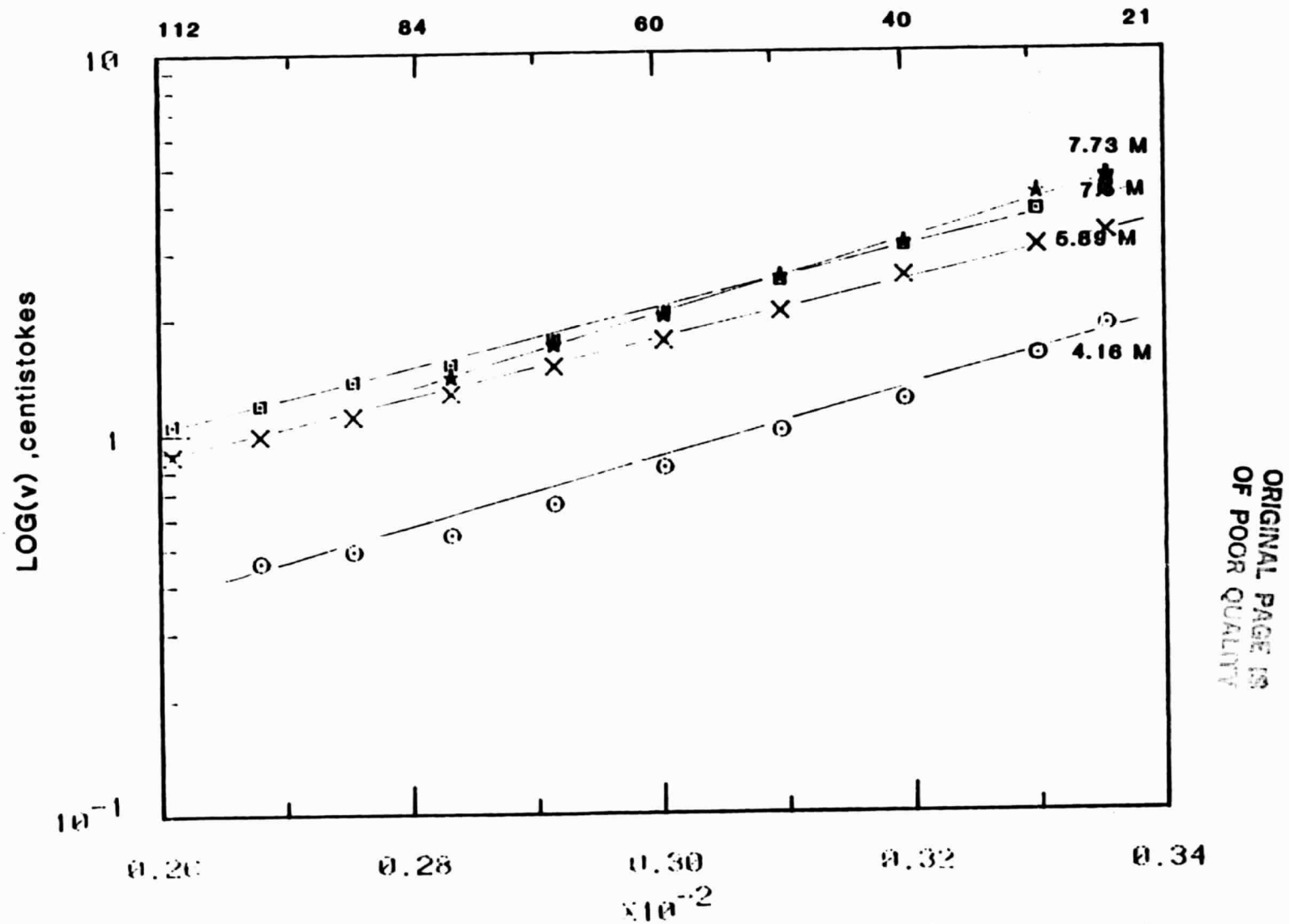

Figure 25 Plot of kinematic viscosity versus reciprocal temperatures at conc. range 4.16 to 7.73 M

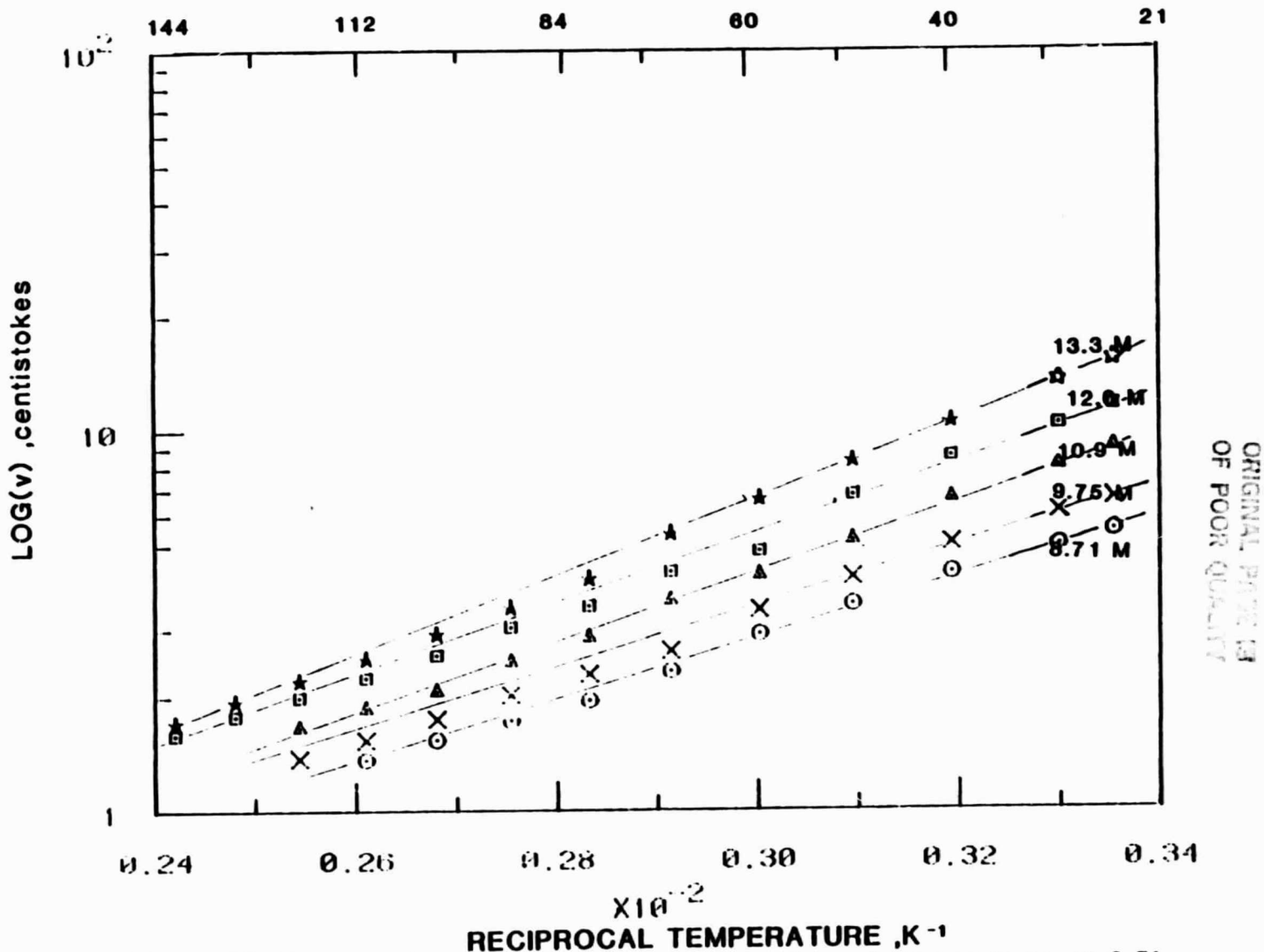

Figure 26 Plot of kinematic viscosity versus reciprocal temperatures at 8.71 to 13.3 M H_3PO_4

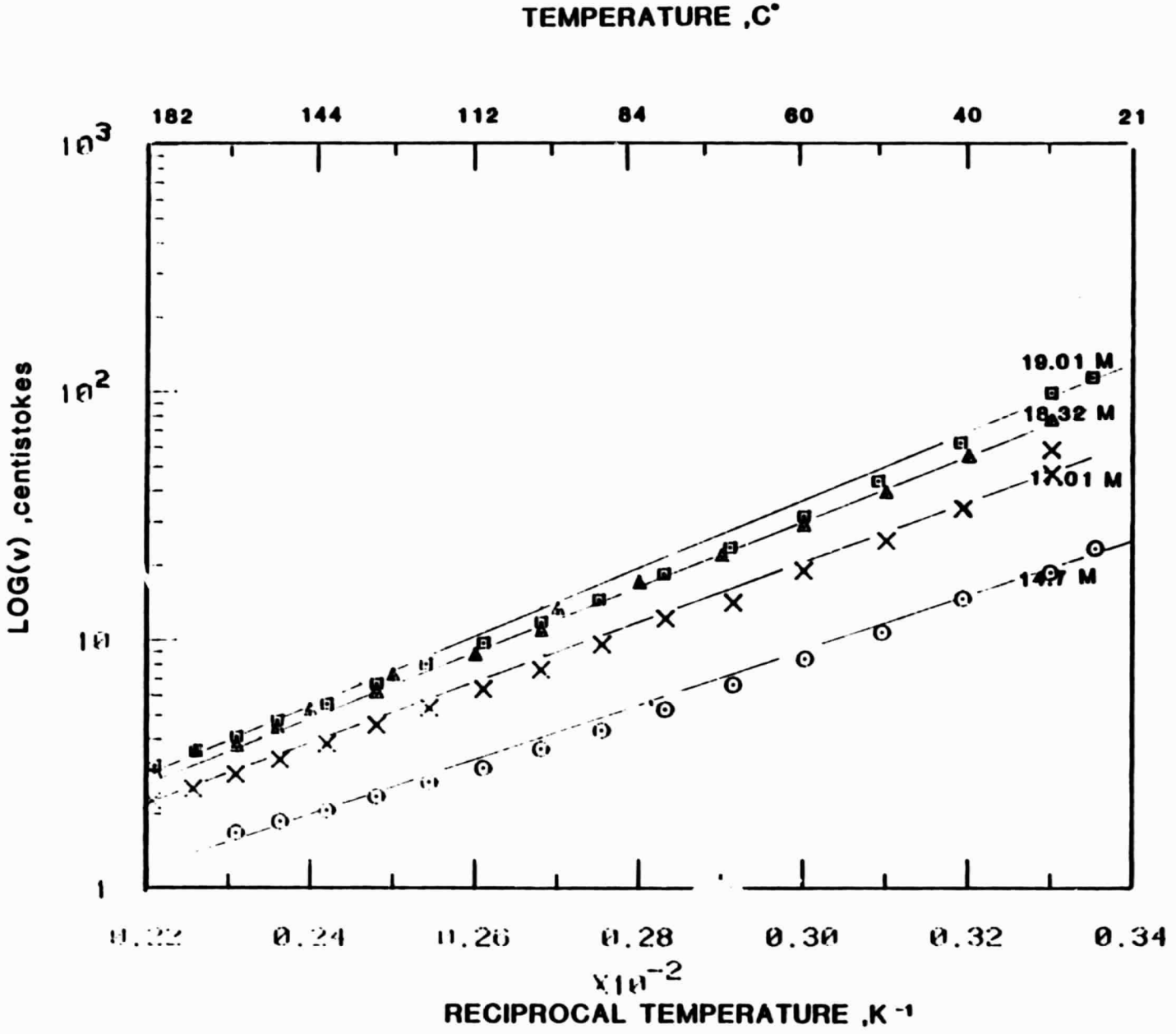

Figure 27 Plot of kinematic viscosity versus reciprocal temperature at concentrates H_3PO_4

3.4 CONCLUSIONS

(1) The electric conductivity of aqueous phosphoric acid solution has been measured over a range of concentrations from 0 to 100%, and temperatures from 25 to 200°C. Attempts were made to correlate the experimental data with the Arrhenius type expression; and the partial success was obtained for the data up to 2.37 M phosphoric acid.

(2) The kinematic viscosity of phosphoric acid as functions of concentraion and temperature was measured for the concentration range of 0-100% and the temperature range of 25-180°C. The data were described by the Arrhenius law.

IV REFERENCES

1. S. Srinivasan, ''Fuel Cell for Electric Utility and Transportation Applications'' Proceedings of the Fifth Australia Electrochemical Conference, Aug. 18-20 (1980).

2. J. O'M. Bockris and S. Srinivasan, ''Fuel Cells: Their Electrochemistry'', McGraw-Hill, N.Y., (1969).

3. S. Sarangapani, P. Bindra, and E. Yeager, ''Physical and Chemical Properties of Phosphoric Acid'', Case Western Reserve University, Cleveland, Ohio. Report to be published on Brookhaven National Laboratory Subcontract.

4. J.W. Harrison and K.M. Parker, ''Molton Carbonate Fuel Cell Design Requirements'', National Fuel Cell Seminar, Norfol, Virginia, June 23-25, (1981).

5. A.O. Isenberg in ''Proceedings of the Symposium on Electrode Materials and Processes for Energy Conversion and Storage'', J.D.E. McIntyre, S. Srinivasan, and F.G. Will, Editors, The Electrochemical Society, Princeton, N.J., 77-6 (1977).

6. K-L. Hsueh, ''Electrode Kinetics of Oxygen Reduction at Platinum in Fuel Cell Electrolytes'', Ph.D. Dissertation, Department of Chemical Engineering, Clarkson College of Technology, Potsdam, N.Y., 13676 (1983).

7. S. Srinivasan, J. McBreen and W.E. O'Grady, ''Survey of Status of Electrode Performance in Phosphoric Acid Fuel Cells'', Final Report. Brookhaven National Laboratory, Upton, N.Y., (1980).

8. W.E. O'Grady, S. Srinivasan and R.F. Dudley, Editors, ''Proceedings of the Workshop on the Electrocatalysis of Fuel Cell Reactions'', vol. 70-2, Electrochem. Soc., Princeton, N.J., (1979).

9. K-L. Hsueh, D-T. Chin, and S. Srinivasan, ''Electrode Kinetics of Oxygen Reduction: A Theoretical and Experimental Analysis of the Rotating Ring-Disk Electrode Method'', J. Electroanal. Chem., 153 (1983) 79.

10. K-L. Hsueh, E.R. Gonzalez, S. Srinivasan, and D-T. Chin, ''Effects of Phosphoric Acid Concentration on Oxygen Reduction Kinetics of Platinum'', J. Electrochem. Soc., accepted for publication.

11. K-L. Hsueh, H.H. Chang, D-T. Chin, and S. Srinivasan, ''Electrode Kinetics of Oxygen Reduction on Platinum in Trifluoromethanesulfonic Adic'', in the ''Proc. Sym. Chem. at Phys. Electrocatalysis,'' the Electro Chem. Soc., in press.

12. A.J. Appleby, ''Oxygen Reduction on Oxide-free Platinum in 85% Orthophosphoric Acid: Temperature and Impurity Dependence'', J. Electrochem. Soc., 117 (1970) 328.

13. A.J. Appleby and B.S. Baker, ''Oxygen Reduction on Platinum in Trifluormethane Sulfonic Acid'', J. Electrochem. Soc., 125 (1978), 404.

14. F. van der Brink, E. Barendrecht and W. Visscher, ''Hydrogen Peroxide as an Intermediate in Electrocatalytic Reduction of Oxygen, A New Method for the Determination of Rate Constant'', J. Electrochem. Soc., 127 (1980) 2003.

15. A. Damjanovic, M.A. Genshow and J. O'M. Bockris, ''Distinction Between Intermediates Produced in Main and Side Electrodic Reactions'', J. Chem. Phys., 45 (1966) 4057.

16. H.S. Wroblowa, Y.C. Pan, and G. Razumney, ''Electroreduction of Oxygen, A New Mechanistic Criterion'', J. Electroanal. Chem., 69 (1976) 195.

17. A.J. Appleby and M. Savy, ''Kinetics of Oxygen Reduction Reactions Involving Catalytic Decomposition of Hydrogen Peroxide'', J. Electroanal. Chem., 92 (1978) 15.

18. R.W. Zurilla, R.K. Sen, and E. Yeager, ''The Kinetics of the Oxygen Reduction Reaction on Gold in Alkaline Solution'', J. Electrochem. Soc., 125 (1978) 1123.

19. V.S. Bagotskii, M.R Tarasevich and V.Yu. Filinovskii, ''Calculation of the Kinetic Parameters of Conjugated Reactions of Oxygen and Hydrogen Peroxide'', Elektrokhimiya, 5 (1969), 1218.

20. E.R. Gonzalez, K-L. Hsueh, and S. Srinivasan, ''The Structure of the Double Layer at the Mercury-Phosphoric Acid Interface from Studies of Adsorption of Thiourea and Its Implications on Oxygen Reduction Kinetics'', J. Electrochem. Soc., 130 (1983).

21. J.C. Huang, R.K. Sen, and E. Yeager, ''Oxygen Reduction on Platinum in 85% Orthophosphoric Acid'', J. Electrochem. Soc., 126 (1979) 786.

22. A.J. Appleby, ''Oxygen Reduction on Active Platinum in 85% Orthophosphoric Acid'', J. Electrochem. Soc., 117 (1970) 641.

23. E.J. Taylor, ''Fundamental Investigations of Fuel Cells for Transportation Applications'', Ph.D. Dissertation, Department of Materials Science, University of Virginia, Virginia (1981).

24. D-T. Chin, ''Technique of Rotating Electrodes for Chemical Analysis'', Bull. Singapore National Inst. of Chem., 9, 35 (1981).

25. A. Damjanovic and V. Brusic, ''Electrode Kinetics of Oxygen Reduction on Oxide-Free Platinum Electrodes'', Electrochim. Acta, 12 (1967) 615.

26. Monsanto Technical Bulletin IC/DP 239.

27. Helmer, Combs and Lafforge, unpublished data of the Monsanto Co., St. Louis, MO.

28. Kakulin, G.P., Fedorchenko, I.A., ''Electrical Conductivity of Concentrated Phosphoric acids at 25-90^{o}C'', Russ. J. Inorg. Chem. 7, 1282 (1962).

29. Fedorchenko, J.A., Kakulin, H.P. and Kondratchenko, Z.V., ''Electrical Conductivity of Concentrated Phosphoric Acids at 100 - 200°C'', Russian J. Inorg. Chem. 10, 1061 (1965).

30 McDonald, D.I. and Boyack, J.R., ''Density, Electrical Conductivity, and Vapor Pressure of Concentrated Phosphoric Acid'', J. Chem. Eng. data 14, 380 (1969).

31. Wydeven, T., ''Electrical Conductivity, of Concentrated Phosphoric Acid from 25 to 60°C'', J. Chem. Eng. data 11, 174 (1966).

32. Greenwood and Thompson, ''The Mechanism of Electrical Conduction in Fused Phosphoric and Trideuterophosphoric Acids'', J. Chem. Soc. 1959 3485, (1959).

33. Greenwood and Thompson, ''Anomalous Conduction in Phosphoric Acid Hemi-hydrate, $2H_3PO_4.H_2O$'', J. Chem. Soc. 1959 3864 (1959).

34. Akiyama, A., Suzuki, T. and Saji, T., ''Electric Conduction and Density of Condensed Phosphoric Acids and their mixtures with Sulfuric Acid'', Bull. Chem. Soc. Japan 45, 146 (1972).

35. Maksimova, I.M., and Yushkevich, V.P., ''Electric Conductivity of Aqueous Solutions of Formic, Acetic, Oxalic, Sulfuric, and Phosphoric Acids at High Temperatures'', Soviet Electrochemistry, 2, 532 (1966).

36. Sarangpamri, S., Bindra, P., Yeager, E., ''Physical and Chemical Properties of Phosphoric Acid'', Report Prepares for the Department of Engergy, unpublished.

37. Gileadi, E., ''Electrochemistry in non-polar media'', A series of two lectures presented at Los Alamos National Laboratory, July 1982.

38. Munson, R.A., ''Self-Dissocaitive Equilibria in Molten Phosphoric Acid'', J. Phys. Chem. 68, 3374, (1964).

39. SaJi, T., Kogyo Kagaku Zaschi 67, 229 (1964).

40. SaJi, T., Kogyo Kagalu Zaschi 68, 609 (1965).

41. Cate, W.E., Deming, M.E., J. Chem. Eng data 15, 290 (1970).

42. Dahlgren, S.E., ''Phorphoric Acid'', Part I, (ed) Slack A.V., Marcel-Dekker, N.Y., Ch. 2, p. 91.

43. Kondratchenko, Z.U., Fedorchenko, I.G., Kovalov, I.Ho, ''Density, Viscosity of Concentrated Phosphoric Acids at 25-90°C'', Russ. J. Inorg. Chem. 4 985 (1959).

44. Kondratchenko, Z.V., Fedorchenko, I.G., Kovalov, I.A., ''Mathematical Calculation of the Density and Viscostiy of Concentrated Phosphoric Acid Solutions'', Russ. J. Applied Chem., 40 1882, (1968).

45. Gubbins, K.E., Walker, Ie., R.D., ''The Solubility and Diffusivity of Oxygen in Electrolytic Solutions'', J. Electrochem. Soc. 112, 469 (1965).

46. Yatskovskii, A.M., Fedotov, N.A., ''Solubility and Diffusion of Oxygen in Solutions of Potassium Hydroxide and Phosphoric Acid'', Russ. J. Phys. Chem. 43, 991 (1969).

47. Klinedinst, K., Bett, J.A.S., McDonald, J. Stonehart, P., ''Oxygen Solubility and Diffusivity in Hot Concentreated H_3PO_4'', J. Electroanal. Chem. 57, 281 (1974).

V NOTATION

Symbol	Description	Unit
a	cross-section area	cm^2
D_1	diffusivity of oxygen	cm^2/S
D_2	diffusivity of hydrogen peroxide	cm^2/S
E	electrode potential	V vs. RHE
Ez	potential of zero charge	V vs. RHE
F	Faraday's constant	C/mol.
I	Cell Current	A
I_d	Disk Current	A
I_{dl}	mass transfer limiting current at disk electrode	A
I_k	kinetic current at disk electrode	A
I_o	exchanging current	A
I_r	ring current	A
J	flux of ions	
K	overall rate constant	cm/S
k	cell constant of a conductivity cell	
ki	rate constant of step i	cm/S
L	specific conductance	mho/cm
l	length of the conductivity medium	cm

Symbol	Description	Unit
m	reaction order of oxygen	
N	collection efficiency	
R	gas constant	J/mol. ^{o}K
R	resistance	ohm
T	temperature	^{o}K
Z_1	$0.62\ D_1^{2/3}\ ^{-1/6}$	$cm/S^{0.5}$
Z_2	$0.62\ D_2^{2/3}\ ^{1/6}$	$cm/S^{0.5}$

GREEK SYMBOLS

c	transfer coefficient	
εeff	energy conversion efficiency	%
χ	specific conductivity	mho/cm
υ	kinematic viscosity	dm^2/S in Ch.2 (centistoke in Ch. 3)
ω	rotating speed of electrode	S^{-1}

VI PUBLICATIONS AND PRESENTATIONS

A. Publication*

1. K-L. Hsueh, D-T. Chin, and S. Srinivasan, ''Electrode Kinetics of Oxygen Reduction: A Theoretical and Experimental Analysis of the Rotating Ring-Disk Electrode Method'', J. Electroanal. Chem., 153 (1983) 79.

2. K-L. Hsueh, E.R. Gonzalez, S. Srinivasan, and D-T. Chin, ''Effects of Phosphoric Acid Concentration on Oxygen Reduction Kinetics at Platinum'', J. Electrochem. Soc., accepted for publication.

3. K-L. Hsueh, H.H. Chang, D-T. Chin, and S. Srinivasan, ''Electrode Kinetics of Oxygen Reduction on Platinum in Trifluoromethanesulfonic Acid'', in the ''Proceedings of the Symposium on the Chemistry and Physics of Electrocatalysis,'' edited by J.D.E. McIntrye, E.B. Zeager and M.J. Weaver, the Electrochemical Society, Inc., Pennington, New Jersey (in press).

B. Presentation

1. K-L. Hsueh, D-T. Chin, and S. Srinivasan, ''Modification of Rotating Ring-Disk Electrode Kinetics to Obtain Rate Constants of Intermediate Steps in Oxygen Reduction'', Electrochemical Society 160th meeting, Denver, Colorado, October 11-16, (1981).

2. K-L. Hsueh, E.R. Gonzalez, and D-T. Chin, ''Effect of the Double Layer Structure on the Oxygen Reduction Kinetics at the Platinum-Phosphoric Acid Interface'', Electrochemical Society 161st meeting, Montreal, Quebec, Canada, May 9-14, (1982).

3. K-L. Hsueh, S. Srinivasan, E.R. Gonzalez, and D-T. Chin, ''Electrolyte Effects on Oxygen Reduction Kinetics on Platinum: A Rotating Ring-Disk Electrode Analysis'', Electrochemical Society, 162nd meeting, Detroit, Michigan, October 17-21, (1982).

4. H.H. Chang, K-L. Hsueh, D-T. Chin, and S. Srinivasan, ''Transport Properties of Phosphoric Acid Fuel Cell Electrolytes'', Electrochemical Society 163rd meeting, San Francisco, California, May 8-13, (1983).

5. K-L. Hsueh, H.H. Chang, D-T. Chin, and S. Srinivasan, ''Electrokinetics of Oxygen Reduction on Platinum in Trifluoromethanesulfonic Acid'', Electrochemical Society 163rd meeting, San Francisco, California, May 8-13, (1983).

---

* A copy of each publication together with an abstract of K-L. Hsueh's dissertation are attached in the Appendix.

6. H.H. Chang, K-L. Hsueh, D-T. Chin, and S. Srinivasan, ''Phosphoric Acid Fuel Cell: Measurement of Transport Properties'', Spring Symposium of the Ontario-Quebec Section of Electrochemical Society, Sherbrooke, Quebec, Canada, April 29, (1983).

7. K-L. Hsueh, H.H. Chang, D-T. Chin, and S. Srinivasan, ''Phosphoric Acid Fuel Cells: Study of Oxygen Reduction Kinetics on Platinum in Trifluoromethanesulfonic and Phosphoric Acid Electrolytes'', Spring Symposium of the Ontario-Quebec Section of Electrochemical Society, Sherbrooke, Quebec, Canada, April 29, (1983).